

To my wife Marg

and temporarily neglected children

Patti and Suzanne

THE RADIATION INITIATED
POLYMERIZATION OF STYRENE

THE RADIATION INITIATED
POLYMERIZATION OF STYRENE

BY

DAVID DEAN, B. Eng.

A Thesis

Submitted to the Faculty of Graduate Studies

in Partial Fulfilment of the Requirements

for the Degree

Master of Engineering

McMaster University

October, 1968

MASTER OF ENGINEERING (1968)
(Chemical Engineering)

McMASTER UNIVERSITY
Hamilton, Ontario

TITLE: The Radiation Initiated Polymerization of Styrene

AUTHOR: David Dean, B. Eng. (McMaster University)

SUPERVISOR: Dean J. W. Hodgins

NUMBER OF PAGES: vii, 120

SCOPE AND CONTENTS: The polymerization of styrene to polystyrene was studied using gamma radiation from a Co^{60} source as the free radical initiator. Conversions up to 50% were obtained and the molecular weight distribution, intrinsic viscosity, bulk viscosity, and osmotic pressure of several samples were measured. A theoretical kinetic model was developed using a slightly modified conventional kinetic scheme and employing a viscosity correction for the termination rate constant. The model predicts conversion over the range studied and molecular weight distributions are in agreement within the limitations of the experimental equipment to measure this parameter.

ACKNOWLEDGEMENTS

The author gratefully acknowledges the encouragement and guidance of Dr. J. W. Hodgins throughout the term of this project. He also wishes to thank fellow graduate students Mr. A. Hui and Mr. S. Balke for their assistance and advice especially in the field of gel permeation chromatography.

The author also wishes to thank Dr. J. Guillet of the University of Toronto for providing space and equipment for the completion of some of the analytical tasks.

TABLE OF CONTENTS

	Page
SUMMARY	ii
ACKNOWLEDGEMENTS	iii
1. INTRODUCTION	1
2. HISTORICAL BACKGROUND	4
2.1 Radiation Chemistry	8
3. THEORY OF POLYMERIZATION KINETICS	12
3.1 Kinetics of Catalyst Free Radicals	13
3.2 Kinetics of Radiation Produced Free Radicals	18
3.3 G_R Value from Kinetic Data	20
3.3.1 G_R for Monomer	20
3.3.2 G_R for Polymer	24
3.4 Conversion - Time Relationship	25
3.5 Molecular Weight Distribution	26
3.6 Influence of Viscosity	29
4. EXPERIMENTAL	31
4.1 Reactor	31
4.2 Analysis	32
4.2.1 GPC	32
4.2.2 Osmometry	32
4.2.3 Intrinsic Viscosity	32
4.2.4 Bulk Viscosity	32
5. EXPERIMENTAL RESULTS	34
5.1 Conversion - Time Data	34
5.2 Viscosity Measurements	39
5.3 GPC Data	39
5.3.1 Universal Calibration Curve	46
5.4 Intrinsic Viscosity	46
5.5 Osmometry	49
5.6 Molecular Weight Distribution	50

	Page
6. DISCUSSION OF RESULTS	52
6.1 Conversion - Time Data	52
6.1.1 Theoretical Conversion - Time Curves	53
6.2 Viscosity Measurements	56
6.3 GPC Data	56
6.4 Universal Calibration Curve	57
6.5 Osmometry	58
6.6 Molecular Weight Distribution	58
7. CONCLUSIONS AND RECOMMENDATIONS	60
7.1 Conclusions	60
7.2 Recommendations	62
8. APPENDICES	
A. Experimental Details	63
A.1 Sample Preparation	63
A.2 Sample Irradiation	66
A.3 Determination of Conversion	69
A.4 Bulk Viscosity Determinations	70
A.5 Polymer Characterization	70
A.5.1 Gel Permeation Chromatography	70
A.5.2 Intrinsic Viscosity	71
A.5.2.1 Experimental	73
A.5.3 Universal Calibration Curve	79
A.5.4 Osmometry	80
A.5.4.1 Experimental	81
B. Dosimetry	83
B.1 Cobalt Glass Dosimetry	84
B.1.1 Experimental	85
B.2 Fricke Dosimetry	88
B.2.1 Experimental	88
C. Solution of Kinetic Equations	94
C.1 Conversion - Time Curve	94
C.2 Viscosity Correction for k_t	95
C.3 Molecular Weight Distributions	96
D. Computer Programs	101

LIST OF ILLUSTRATIONS

		Page
FIG.3.1	G_R as a Function of Dose-Rate	22
3.2	Effect of G_R on Theoretical Conversion	26 a
5.1	Thermal Polymerization of Styrene	37
5.2	Conversion - Time Data	38
5.3	Effect of G_R^m and G_R^p on Theoretical Conversion	40
5.4	Best Theoretical Fit of Experimental Data	41
5.5	Bulk Viscosity vs Irradiation Time	42
5.6	Viscosity vs Irradiation Time and Polymer Weight Fraction	43
5.7	Universal Calibration Curve	47
5.8	Polymer Weight Fraction vs Chain Length	51
A.1	Reaction Vial	64
A.2	Sample Holder and Agitator	67
A.3	Ubbelohde Dilution Viscometer	74
A.4	Viscosity Number vs Concentration	76
A.5	Intrinsic Viscosity vs Molecular Weight	78
A.6	Osmotic Pressure - Concentration Plot	82
B.1	Vial Holder for Fricke Dosimetry	90
C.1	Logic Diagram for Radiation Reactor Program	100

LIST OF TABLES

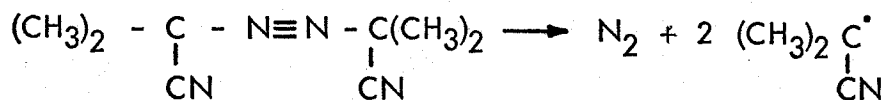
		Page
5.1	Irradiation Time - Conversion Data for Agitated Samples	35
5.2	Irradiation Time - Conversion for Non-Agitated Samples	36
5.3	GPC Data - Agitated Samples	44
5.4	GPC Data - Non-Agitated Samples	45
5.5	Standards for Universal Calibration Curve	46
5.6	Intrinsic Viscosities and Calculated \bar{M}_v	48
5.7	Comparison of Molecular Weight Determinations	49
A.1	Styrene Analysis	65
A.2	Intrinsic Viscosities of Standard Samples	79
B.1	Dose Rate from Cobalt Glass Dosimetry	87
B.2	Dose Rate from Fricke Solution Dosimetry	92

1. INTRODUCTION

Studies on reactor designs for producing polystyrene by free radical catalysis show that deviations between theoretical conversions of monomer to polymer and the experimental results occur mainly for bulk polymerization and at high conversions. Theoretically predicted molecular weight distributions are also in error under these conditions as shown by Tebbens⁽¹⁾ using gel permeation chromatography for analysis. The present work was undertaken, in part, to study the conversion of styrene to the polymer in bulk, using a free radical generation system which would be free of the catalyst efficiency problems encountered by other workers.

A considerable amount of work has been done on the study of the polymerization of styrene by ionic mechanisms and by free radical mechanisms. In the latter case the reaction is usually catalysed by azobisisobutyronitrile although many other catalysts such as benzoyl peroxide, metallic halides and ozonides which decompose readily to form free radicals, have been used⁽²⁾.

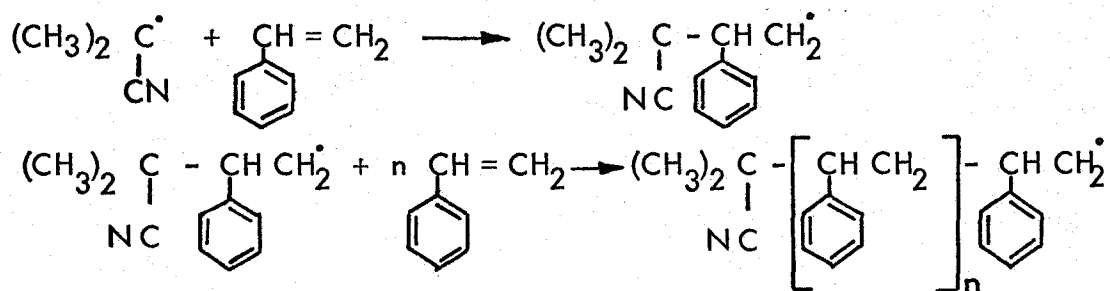
In the case of azobisisobutyronitrile the decomposition reaction as shown below can be followed by the amount of nitrogen produced.



Consequently, the rate of free radical production can be determined as a function of temperature.

In the polymerization reaction, the catalyst free radical reacts with the

double bond of the styrene molecule producing a new radical which is free to react with other monomer molecules.



The kinetics of this reaction together with the termination reactions which produce the final polymer have been studied extensively. Most recently, bulk and solution studies have been made using gel permeation chromatography to analyse molecular weight distributions and a high speed digital computer for the solution of the theoretical equations. Good agreement between theoretical and experimental results has been found in most cases⁽¹⁾.

A major problem in studying the kinetic equations involving azo catalyst is the apparent variation in catalyst efficiency i.e. the measure of the number of catalyst free radicals which actually initiate a polymer chain. Furthermore, the rate of free radical production is first order in catalyst concentration and may be written as

$$-\frac{dc}{dt} = k_d C \quad \text{where } C \text{ is catalyst concentration.}$$

Obviously as the reaction proceeds and catalyst is consumed, the rate of free radical production varies and complicates the overall kinetics.

In undertaking the present study, it was considered advantageous to have a means of free radical production which would be constant throughout the total time of the reaction and independent of factors such as catalyst efficiency and

monomer concentration. However, to be of more direct commercial interest it was also considered desirable to study fairly high conversions (up to 65%). High energy gamma radiation was selected as the radical initiator since the rate of production of monomer free radicals would be constant because of the constant emission of high energy photons from a radioactive source such as Co^{60} . Unfortunately, the decision to study high conversions introduces many complicating factors both in the theoretical predictions of the kinetics and in characterization of the polymer produced in these studies.

This study was in part, prompted by the availability of a gel permeation chromatograph to give rapid analysis of the molecular weight distribution of the material formed by irradiation of the styrene monomer. A knowledge of the distribution is essential for an accurate prediction of the kinetic mechanisms.

2. HISTORICAL BACKGROUND

Ever since styrene was separated from "natural balsamic material - storox" in 1839 by E. Simon⁽³⁾, its ability to polymerize readily or form a jelly-like material has been noted. Although Simon was the first to name the monomer (he called it styrol) it appears that prior to 1786, a chemist by the name of Neuman actually performed experiments with storox and separated an "essential oil" which in all probability was styrene⁽⁴⁾. Dragon's blood, a resin from the Malayan rattan palm, was another early source of styrene.

The increased demand for synthetic rubber during the early 1940's greatly accelerated styrene production and most styrene produced since that time has been by the catalytic dehydrogenation of ethylbenzene.

The polymer produced by Simon in 1839 was originally thought to be an oxidation product and was named "styrol oxide", but this was proved incorrect by Blyth in 1845⁽⁵⁾. Ostromislensky and later Staudinger⁽⁶⁾ about 1920 advanced important ideas about the mechanism of the polymerization reaction and most significantly that the polymer consisted of a large number of styrene monomer units connected through their vinyl groups. Staudinger suggested the name polystyrene for the compound.

Polystyrene is an extremely important commercial product because of its low cost, excellent moldability, good dimensional stability, chemical inertness, good electrical properties, ease of colouring and ability to form copolymers. However, its physical properties are in large measure dependent on such factors

as average molecular weight, molecular weight distribution, and chain geometry. It is very important, therefore, that the conditions affecting these factors be known and controlled if possible during polymer manufacture.

Styrene is readily converted to the polymer by heat, proceeding slowly at room temperature but requiring only a few hours above 150°C. As the rate of the polymerization reaction increases the average molecular weight decreases tending to produce a weak and brittle material⁽⁷⁾. This is also true of peroxide catalyzed polymerizations. Only in the case of emulsion polymerization can the rate of reaction and molecular weight be varied independently.

Methods for determining molecular weight and molecular weight distributions for polystyrene have been a problem for some time. However, some reasonably accurate techniques have been employed, notably by Staudinger in his dilute solution viscosity determinations and modified by Kraemer and Lansing⁽⁸⁾ with the concept of intrinsic viscosity. Attempts to determine the molecular weight distribution of a heterogeneous polymer sample led Lansing and Kraemer⁽⁹⁾ to define the terms number average \bar{M}_n , weight average \bar{M}_w , and Z average \bar{M}_z , molecular weight which in practice represent successive moments of the distribution curve obtained by plotting the weight fraction of polymer against polymer chain length. The ratio of weight average to number average molecular weight \bar{M}_w / \bar{M}_n gives an indication of the spread of the curve with a truly monodispersed sample giving $\bar{M}_w / \bar{M}_n = 1$.

Sedimentation methods such as those employed in the ultracentrifuge have been used for some time to determine molecular weight distributions but only

recently have instruments and evaluation techniques become sufficiently refined to make this suitable for routine analysis. One major problem still associated with ultracentrifuge work is the slowness in completing a sample characterization.

Although the actual Schlieren photographs of the settled material can be obtained in about one hour, several days work is required to extract the essential data from these photographs and obtain a molecular weight distribution. Another difficulty is the inability of the instrument to handle samples of wide variation in molecular weight, or samples with molecular weights much less than one hundred thousand.

Since 1936⁽¹⁰⁾ chromatographic methods of separation have been studied with varying degrees of success. These studies can be divided broadly on the basis of the solvent employed namely into aqueous and organic systems⁽¹¹⁾. Bolding⁽¹²⁾ in 1959 used swollen rubber to separate mixtures of fatty acids and in 1960 Vaughan⁽¹³⁾ fractionated polystyrene by "gel filtration" using a column packing of insoluble cross-linked polystyrene with different degrees of swelling and benzene as eluant. In 1962 two important advances in the field were reported. The first was Moore's⁽¹⁴⁾ process for making highly cross-linked, rigid gels with a wide range of permeabilities. The second was the use of a differential refractometer as a continuous detector of polymer concentration in the eluant. The term "gel permeation chromatography" (GPC) was coined at approximately this time. These developments led in 1964 to the production of a commercial instrument by Waters Associates, Inc.

Although the GPC provides the most rapid method yet developed for determining molecular weight distributions, it is by no means the answer to all

problems in this area. Recent work by Benoit et al⁽¹⁵⁾ using linear and branched polymers claims the important parameter for retention time in the GPC is the hydrodynamic volume of the macromolecules which may in fact be independent of the molecular weight, particularly in a highly branched molecule. Linear and branched molecules possessing the same hydrodynamic volume would have the same column retention time, hence no universal relationship between retention time and molecular weight would exist.

A universal calibration curve suggested by Benoit could apply to linear or branched molecules. When $\log [\eta] M$ is plotted against elution volume, where $[\eta]$ is the intrinsic viscosity of the polymer and M is molecular weight, both branched and linear molecules fit the same curve. If the exact structure of a branched molecule was known and a similarly branched standard of known molecular weight was run on the GPC, then the universal calibration curve would serve to predict the molecular weight of the unknown. This, however, is not a very practical situation and the most likely probability is that branched samples will only be characterized as corresponding to a particular molecular volume and not molecular weight. This would result in a molecular size distribution which might be a useful parameter.

Two other methods widely used for gaining information about polymer molecular weights are osmometry and light scattering. A membrane osmometer which actually counts numbers of solute molecules present in a solution will allow a direct determination of the number average molecular weight \bar{M}_n . Light scattering, on the other hand, depends upon the concentrations and molecular

weight of scattering particles hence will give a weight average molecular weight \bar{M}_w . If both \bar{M}_n and \bar{M}_w are known it is possible to make some predictions about the actual distribution curve⁽¹⁶⁾. Possibly a molecular size distribution from the GPC coupled with \bar{M}_n and \bar{M}_w determined by osmometry and light scattering could be used to determine the molecular weight distribution for cross-linked and branched polymers.

2.1 Radiation Chemistry

The use of high-energy radiation to initiate polymerization reactions has developed extensively only since World War II and much of the early work gives conflicting results through an apparent lack of knowledge of the influence of many important factors, such as temperature, presence or absence of oxygen, and purity of reagents⁽¹⁷⁾.

The term "high-energy radiation" or "ionizing radiation" refers to a host of different types of radiations capable of producing ions directly or indirectly in a medium of common elements, such as air or water. Electromagnetic waves such as X-rays or gamma rays are not capable of producing ions directly but can transfer their energy to electrons which create secondary tracks of ions. Since the ionization potentials of elements such as nitrogen and oxygen are in the 10 to 15 eV range, the lower limit of the energy range for high-energy radiation can be defined in this way. The effective upper limit depends upon the type of radiation and its source. In the case of gamma radiation from a Co^{60} source, there are two strong gamma photons with energies of 1.177 Mev

and 1.332 Mev. For a complete summary of radiation sources and energies see reference (18).

Although the energy per photon determines whether or not the radiation will be capable of breaking a chemical bond, the important question of yield depends upon two factors. First is the intensity of the radiation source i. e. the number of photons emitted per unit time. Second, is the number of active chemical species produced per photon of radiation. In the latter case a chemical chain reaction initiated by a single photon of radiation may produce several thousand new molecules.

Intensity of Radiation :

The intensity of a beam of radiation is defined as the energy flowing through unit area perpendicular to the beam per unit time. It is usually expressed in ergs per square centimeter-second or watts per square centimeter⁽¹⁹⁾.

Since all "ionizing radiation" passing through matter does not interact with the matter, a measure of the energy of the radiation beam actually interacting is called the "absorbed dose". The official unit of absorbed dose is the "rad".

$$1 \text{ rad} \equiv 100 \text{ ergs/gram} \equiv 6.25 \times 10^{13} \text{ e.v./gram.}$$

All matter does not interact in the same way with the radiation beam. The interdependence between the two is expressed in the absorption coefficient μ according to the relationship:

$$I = I_0 e^{-\mu x}$$

where I is the intensity of the beam after passing through the material, I_0 the original intensity, and x the thickness of the absorbing material.⁽²⁰⁾

G Value:

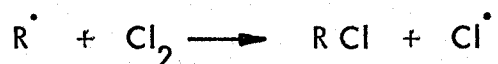
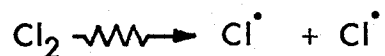
The measure of the number of new chemical species produced as a direct result of interaction of matter with radiant energy is expressed by the term "G value". For the production of new molecules by this process the definition would be:

$$G = \frac{\text{no. of new molecules produced}}{100 \text{ e. v. of absorbed energy}}$$

For the production of free radicals in a hydrocarbon system the symbol G_R is used. It may have a wide range of actual values but is usually between 0.01 and 10.0 for hydrocarbons with the lower values for aromatic systems and the higher values for aliphatic systems. The lower value for the aromatic compounds is apparently the result of resonance energy absorption by the benzene ring which stabilizes the molecule against breaking of a C-H bond.

In vinyl monomers such as styrene the increased resonance of the double bond further stabilizes the molecule giving G_R values for the polymer approximately three times greater than for those of the monomer.

If the radiation initiates a chain reaction in the system with which it interacts, such as the chlorination of methane⁽²¹⁾, the G value of the reaction may be as high as 3.0×10^6 or greater. An example of such a chain reaction is shown below.

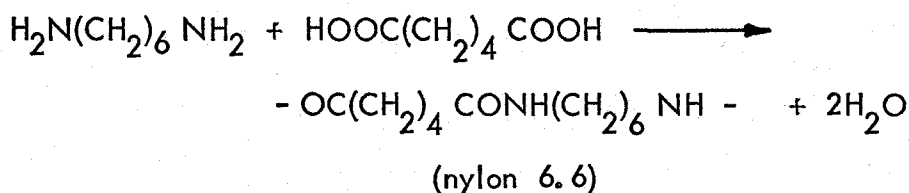


In this case, free radicals started by the original irradiation could continue producing the species R Cl until termination occurred by radical-radical interaction.

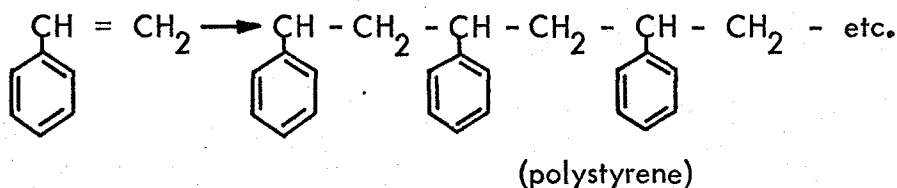
Since radiation sources are a relatively expensive means of providing energy for a chemical reaction, any commercial processes utilizing these sources must have a high G value for the reaction as in a chain reaction or a large weight yield per molecule produced as in the case of polymer production. In the latter case a modest G value could still yield a high ratio of weight of product produced / energy absorbed, since molecular weights may be a million or greater.

3. THEORY OF POLYMERIZATION KINETICS

Polymerization reactions are categorized as either condensation reactions or addition reactions. In a condensation polymerization such as hexamethylene diamine and adipic acid to produce nylon 6.6, a small molecule, such as water is produced in addition to the polymer molecule.



In addition polymerization, as occurs with vinyl compounds, the molecular formula of the polymer is identical with that of the monomer⁽²²⁾.

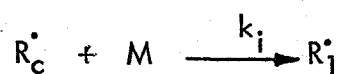
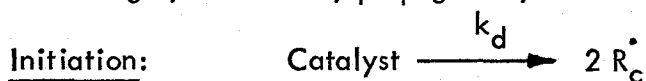


Addition reactions such as the polymerization of styrene may take place by a free radical mechanism or under some circumstances by an ionic mechanism. Metal halides are generally used to catalyze ionic polymerizations but these require a co-catalyst, the most important of which is water⁽²³⁾. Oddly enough, when ionic polymerization is initiated by radiation, the presence of water inhibits the reaction. When conditions have been specifically designed to prevent a free radical mechanism from operating, such as low temperatures (-78°C) and the addition of radical scavengers, the resulting polymerization can be attributed to an anionic mechanism^(24,25). Conversely, when reaction conditions are

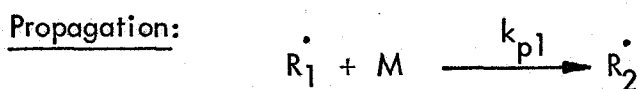
designed, as they were in this work, to give relatively high temperatures (50°C) and using styrene saturated with water, there is no possibility that an ionic mechanism was operative.

3.1 Kinetics of Catalyst Free Radicals

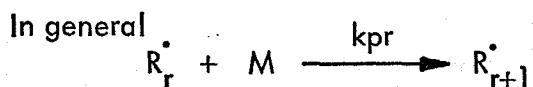
The free radical polymerization reaction can be divided into three stages; initiation, propagation, and termination.



For azobisisobutyronitrile as catalyst and styrene as monomer the above reaction is shown in detail on pages 1 and 2.



where R_2^\bullet represents a radical of the form R_1M^\bullet



As a growing polymer free radical adds monomer units the chain length rapidly increases and it is referred to as a live polymer chain.

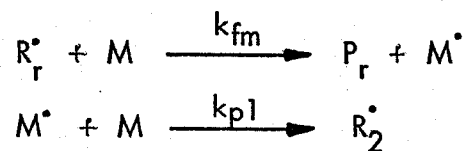
The length to which any one chain grows is unpredictable but the average chain length is a function of reaction conditions.

Transfer:

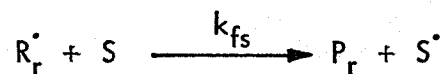
A collision between a free radical and any other molecule in the system may result in a transfer of the active centre from one molecule to the other. Although this transfer reaction may halt the growth of a

particular polymer chain the free radical may continue to initiate other chains; hence the free radical concentration is unaffected by this process.

For example:



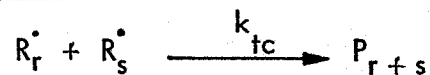
The dead polymer P_r could possibly be reactivated to a growing chain if it reacts with another free radical. In solution, transfer could also occur between solvent molecules and polymer free radicals.



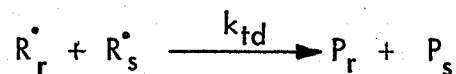
This reaction still does not affect the overall free radical concentration in the system.

Termination: Growth of the polymer chain terminates either by combination or disproportionation. Both processes require a reaction between two free radicals.

Combination



Disproportionation



In disproportionation a hydrogen atom from one live polymer chain is transferred to another, thereby terminating both chains but leaving one with a double bond.

A number of simplifications are generally applied to the kinetic equations given above which have been found by experimentation to be

justified in all but special cases⁽²⁶⁾. The first of these is that the rate of propagation is independent of the chain length of the live polymer, hence

$$k_{p1} = k_{p2} = \dots = k_{pr} = k_p$$

Similarly k_f , k_{tc} , and k_{td} are independent of chain length.

Secondly, it is assumed that the consumption of monomer in the initiation or transfer reactions is negligible compared to that consumed during propagation, hence

$$-\frac{d[M]}{dt} = k_p [M] [R^\bullet] \quad \text{where } [R^\bullet] = \sum_{r=1}^{\infty} [R_r^\bullet] \quad (1)$$

From the foregoing equations the rate of change of $[R_1^\bullet]$ would be:

$$\begin{aligned} \frac{d[R_1^\bullet]}{dt} = & I - k_p [M] [R_1^\bullet] + (k_{fs} [S] + k_{fm} [M]) [R^\bullet] \\ & - (k_{fs} [S] + k_{fm} [M]) [R_1^\bullet] - (k_{tc} + k_{td}) [R_1^\bullet] [R^\bullet] \end{aligned} \quad (2)$$

where I is the rate of formation of R_1^\bullet .

For $[R_2^\bullet]$ and higher it would be:

$$\begin{aligned} \frac{d[R_r^\bullet]}{dt} = & k_p [M] [R_{r-1}^\bullet] - k_p [M] [R_r^\bullet] - (k_{fs} [S] + k_{fm} [M]) [R_r^\bullet] \\ & - (k_{tc} + k_{td}) [R_r^\bullet] [R^\bullet] \end{aligned} \quad (3)$$

The rate of formation of polymer of chain length r would be:

$$\begin{aligned} \frac{d[P_r]}{dt} = & (k_{fs} [S] + k_{fm} [M]) [R_r^\bullet] + k_{td} [R_r^\bullet] [R^\bullet] \\ & + 1/2 k_{tc} \sum_{n=1}^{r-1} [R_n^\bullet] [R_{r-n}^\bullet] \end{aligned} \quad (4)$$

The third assumption is that a stationary state is rapidly established and maintained throughout the reaction with respect to the concentration of radical intermediates. This may be shown as

$$\frac{d [R^\bullet]}{dt} = 0 \quad (5)$$

When this assumption is applied to equations (1), (2), and (3) with the intermediate polymer chains also considered, each equation can be set equal to zero. Summing these equations then leads to the result

$$I = k_t [R^\bullet]^2 \quad (6)$$

This may also be written directly if I represents the rate of appearance of monomer free radicals and if all disappear by termination then

$$\frac{d [R^\bullet]}{dt} = I - k_t [R^\bullet]^2 \quad (7)$$

When a catalyst such as azobisisobutyronitrile is used to produce the free radicals the first order reaction may be written

$$-\frac{dC}{dt} = k_d C \quad (8)$$

where C is catalyst concentration

Thus if C_0 represents the initial catalyst concentration

$$C = C_0 e^{-k_d t} \quad (9)$$

To relate this to I , the rate of generation of free radicals, it is necessary to consider an efficiency factor since all catalyst free radicals do not succeed in propagating a polymer chain.

$$I = 2fk_d C = 2fk_d C_0 \exp(-k_d t) \quad (10)$$

Using the steady state assumption, equation (7) becomes

$$[R^*] = \left[\frac{I}{k_t} \right]^{1/2} \quad (11)$$

If the initial monomer concentration is $[M_0]$ and the conversion is defined as X , then

$$[M] = [M_0] (1 - x) \quad (12)$$

and from equation (1)

$$\frac{dx}{dt} = k_p (1 - x) [R^*] \quad (13)$$

Combining equations (10) and (11) with this result gives

$$\frac{dx}{dt} = k_p (1 - x) \left[\frac{2f k_d C_0 \exp(-k_d t)}{k_t} \right]^{1/2} \quad (14)$$

The solution of this equation gives conversion as a function of time and initial catalyst concentration provided a satisfactory value of "f" and the rate constants can be found. This is not always an easy matter since a wide variation in values have been reported in the literature⁽²⁷⁾.

Furthermore, it is likely that "f" is a function of monomer concentration and viscosity. De Schrijver and Smets⁽²⁸⁾ have shown that although the rate of decomposition of the catalyst is not affected by viscosity the efficiency can be reduced as much as 50% on increasing the viscosity.

If we assume that f , k_t , k_p , and k_d are constant the analytical solution of (14) from time zero to t yields

$$\ln(1 - x) = \sqrt{\frac{8 f k_p^2 C_0}{k_d k_t}} \exp(-k_d t / 2) \quad (15)$$

Hui⁽²⁹⁾ allowed for variation in f and k_t by treating both as functions of

viscosity. The constants k_p and k_d are not viscosity dependent hence no corrections were made for these. Equation (14) can still be solved under these circumstances if f and k_t are considered constant over a small interval from time t_1 to t_2 and the ratio f/k_t is corrected at each step. Then the conversion x_2 is given by

$$x_2 = 1 - \exp \left\{ \ln(1 - x_1) + \sqrt{\frac{8 f k_p^2 C_o}{k_d k_t}} \left[\exp\left(-\frac{k_d t_2}{2}\right) - \exp\left(-\frac{k_d t_1}{2}\right) \right] \right\} \quad (16)$$

Using an initial catalyst efficiency of 0.6 and

$$k_d = 1.58 \times 10^{15} \exp(-15500/T)$$

$$k_p = 1.051 \times 10^7 \exp(-3557/T)$$

$$k_t = 1.255 \times 10^9 \exp(-844/T)$$

for the solution of (16), Hui got good agreement between theoretical and experimental results for conversions up to 60% in solution polymerization.

3.2 Kinetics of Radiation Produced Free Radicals

The primary difference between catalyst generated and radiation generated free radicals is the nondiscriminatory nature of the radiation process. With high energy gamma radiation any intramolecular bond can be broken to generate free radicals in either monomer, polymer, or solvent molecules. The rate at which the radicals are generated however, will in general be different for different substances. If bulk polymerization alone is considered, the only source of free radicals initially is the monomer.



From this point on the radical interactions are the same as those outlined for the catalyst system except that no catalyst fragments would appear as end groups in polymer chains. The rate of production of free radicals in moles per litre per unit time may be written as:

$$R_i = \phi_m [M] I_r \quad (17)$$

where $\phi_m [M]$ is the rate of production of radicals in the monomer expressed in moles per litre per unit radiation dose and I_r is the dose-rate usually expressed in rads per unit time. The rad is defined on page 9. I_r is equivalent to the rate of catalyst decomposition in the catalysed system except that I_r is relatively constant varying only slightly as the strength of the radiation source gradually deteriorates. The actual value of the absorbed dose can be determined by any of several methods of dosimetry. Two of these methods used in this work are described in appendix B.

The term $\phi_m [M]$ is equivalent to the G_r value which is defined on page 10. As shown in equation (1), for the condition when the propagation step is the primary consumer of monomer, and when steady state conditions exist (i. e. $R_i = k_t [R^\bullet]^2$), the overall reaction rate is:

$$R = k_p [R^\bullet] [M] = \frac{k_p}{k_t^{1/2}} R_i^{1/2} [M] \quad (18)$$

or in terms of dose rate:

$$R = \frac{k_p}{k_t^{1/2}} (\phi_m [M] I_r)^{1/2} [M] \quad (19)$$

Equation (18) is the classical free radical kinetic equation showing the

reaction rate proportional to the square root of initiation. Experimental evidence of deviations from this equation were gained for the first time from radiation studies of polymerization.^{(30) (31)} When rates of initiation are very high and all free radicals produced do not get rapidly converted into growing chains a more complete kinetic scheme must be employed. For details of the complete kinetics see reference (32).

Chapiro and Wahl⁽³⁰⁾ studied the polymerization of styrene at dose rates from 0.006 to 7.3 rads per sec and at the highest dose-rates they found the dose-rate exponent of equation (19) decreased below the value of one half. This result was interpreted by assuming the monomer could not react with all the primary radicals formed at the higher dose-rates and that some of the radicals recombined without initiating polymer chains.

Since the dose-rate used in the present work was approximately 200 rads per sec it would be expected that deviations from the predicted rate equations observed by Chapiro and Wahl would be even more evident. The difficulty in getting a true measure of this effect is in knowing what value to use for the term $\Phi_m [M]$ since this value is usually estimated by first assuming a kinetic model.

3.3 G_r Value from Kinetic Data

3.3.1 G_r for Monomer

By definition G_r is the number of free radicals produced per 100 e. v. absorbed by the species. The value of G_r has been estimated by using free radical scavengers such as benzoquinone

or diphenylpicrylhydrazyl. If the concentration of the scavenger is accurately known and the time for which the scavenger will effectively inhibit polymerization is also known, then the number of free radicals produced during that time period can be determined.

A more common method of estimating G_r is from kinetic data but this method has the serious limitation that the answer derived is meaningful only if the kinetic assumptions are accurate.

From equation (17), $\Phi_m [M]$ represents the number of free radicals produced, expressed in moles per litre per rad i. e. moles per litre per 6.25×10^{13} e. v. per gram, when the dose rate I_r is expressed in rads per second. Then the relationship

between G_r and $\Phi_m [M]$ would be:

$$G_r = \frac{\Phi_m [M] \times 6.02 \times 10^{23}}{6.25 \times 10^{11} \times \text{Density (gm/litre)}} \quad (20)$$

The density of styrene at 50°C is 0.8800 gm/ml,

thus

$$G_r = 1.095 \times 10^9 \Phi_m [M] \quad (21)$$

Combining this result with equation (19), gives

$$G_r = (1.095 \times 10^9) \frac{k_t}{k_p^2} \left(\frac{R}{[M]} \right)^2 I_r^{-1} \quad (22)$$

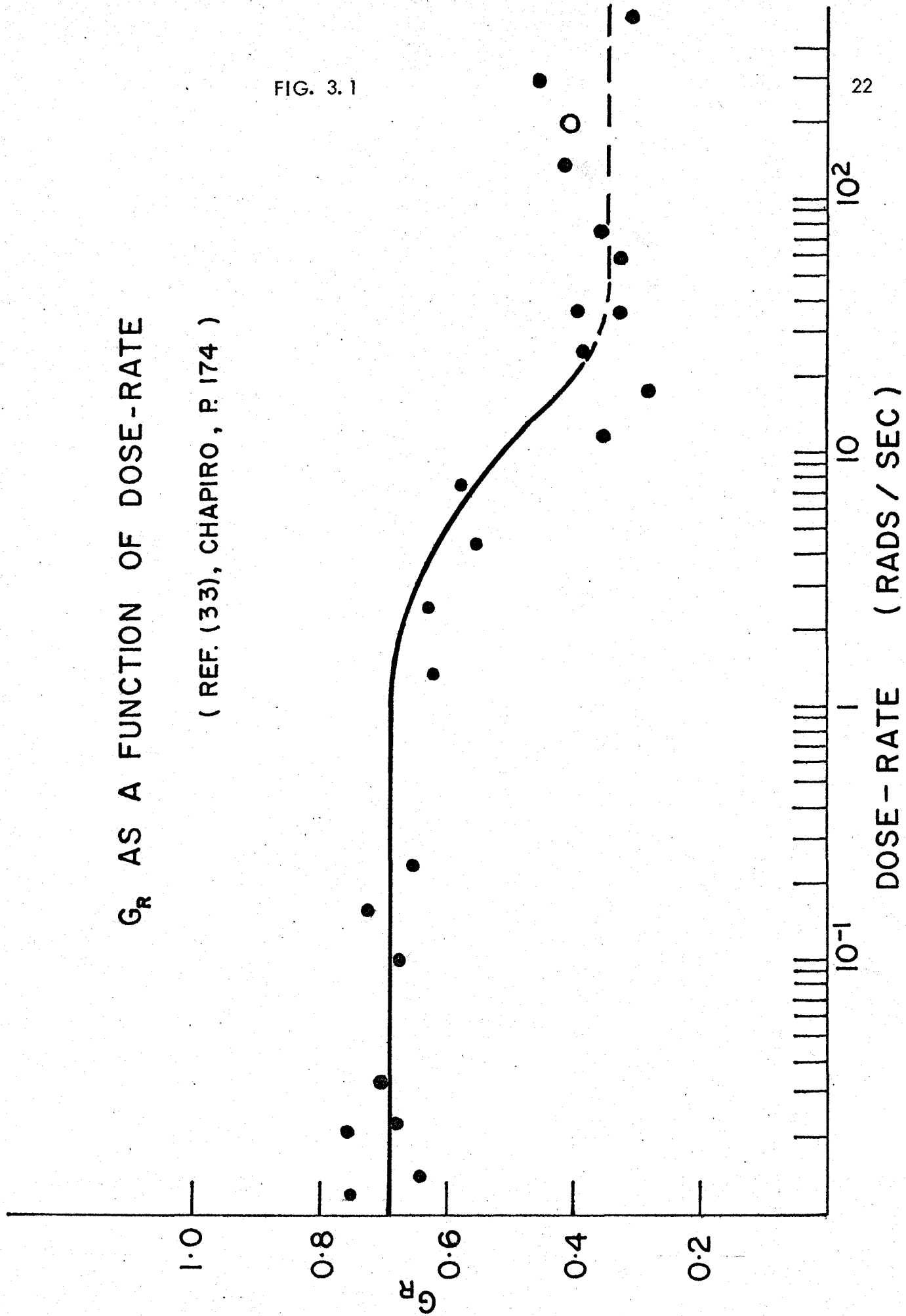
Since R , M , and I_r are interrelated the G_r value from equation (21) should be a constant if k_t and k_p are constant.

A plot of G_r vs dose-rate (Figure 3.1) shows that G_r is a

G_R AS A FUNCTION OF DOSE-RATE

(REF. (33), CHAPIRO, P. 174)

FIG. 3.1



constant for dose-rates up to about 2 to 3 rads per second but then drops to a lower value at higher dose-rates. Chapiro⁽³³⁾ has pointed out that this apparent decrease in G_R is probably due to the fact that above some critical value of dose-rate the simplified kinetic picture used to calculate G_R is no longer applicable.

Since it is difficult to conceive of any theoretical reason why the number of free radicals produced per 100 e. v. of energy absorbed by the species should be dependent upon the rate at which that energy is being supplied to the system, Chapiro's explanation for the reported changes in G_R seems quite reasonable.

Using the value of k_t and k_p from page 18 at 50°C the ratio k_t/k_p^2 has the value 3.02×10^3 . For the present work I_r was 194 rads per sec and R was constant over the range of the experiment with a value of 4.14×10^{-5} moles / litre / second. (See Section 5 for details of experimental results). Equation (21) then yields a value for G_R of 0.40 .

Referring to figure 3.1 this value for G_R falls well within the scatter of experimental points reported by other workers who have also assumed the simplified kinetic equations are applicable. Since the dose-rate values above 100 rads / sec in figure 3.1 were generated with 400-500 kv X-rays⁽³⁴⁾, this work shows some consistency between gamma ray and X-ray initiated

polymerization.

If we assume, as previously discussed, that the lower G_R values are in error because of over simplification of the kinetics, then it would be reasonable to use the higher value of 0.69 (reported by Chapiro⁽³³⁾) in further calculation.

3.3.2 G_R for Polymer

The previous section has considered the production of free radicals in the monomer only. In section 2, it was pointed out that polymer molecules are more likely to form free radicals when subjected to high energy radiation than are monomer molecules since the polymer has less resonance stabilization. It would be expected, therefore, that when the concentration of polymer in the system became appreciable a noticeable change in the overall G_R value would result. Unfortunately, little information is available on the G_R value of most polymers although estimates have been made of these values by comparison with low molecular weight material of similar chemical structure. For polystyrene, an estimated value from isopropylbenzene and xylene is given by Chapiro⁽³⁵⁾ as 1.5 to 3.0. This value is between two and one half to four and one half times the G_R value of the monomer.

When chain initiation by polymer radicals takes place, the resulting chains would have higher molecular weights than the monomer initiated chains. In addition, the chains are just

as likely to initiate on the side of a molecule as they are on the end, resulting in a branched polymer.

The rate of initiation would necessarily increase as the percentage of polymer in the system increased and equation (17) would be modified to

$$R_{it} = (\phi_m [M] + \phi_p [P]) I_R \quad (23)$$

where $\phi_p [P]$ is the rate of production of free radicals in the polymer expressed in moles per litre per unit radiation dose.

A further complicating factor in predicting increases in molecular weight due to polymer free radical production is the possibility of chain scission. Although polystyrene is generally regarded as a cross-linking polymer it is only possible to say that it cross-links in greater yield than it degrades. This can be compared with Teflon which is classed as a degrading type polymer although evidence⁽³⁶⁾ suggests that it may also cross-link.

3.4 Conversion - Time Relationships

Ballantine et al⁽³⁷⁾ using a dose rate of 64 rads/sec at 72°C reported a linear relationship for percent conversion of styrene to polymer vs. time up to approximately 65% conversion. Beyond this point the curve rose sharply and then levelled off as it approached 100% conversion. This effect was also reported by Landler⁽³⁸⁾.

The theoretical conversion-time relationship can be obtained from equation (22). Rearranging this equation yields

$$R = -\frac{d[M]}{dt} = \frac{k_p}{k_t^{1/2}} \left[\frac{G_R I_R}{1.095 \times 10^9} \right]^{1/2} [M] \quad (24)$$

If the value of $k_p / k_t^{1/2}$ and $G_R I_R$ are relatively constant over some finite time interval t_1 to t_2 then equation (24) can be integrated to give

$$\ln \frac{[M_2]}{[M_1]} = -\frac{k_p}{k_t^{1/2}} \left[\frac{G_R I_R}{1.095 \times 10^9} \right]^{1/2} (t_2 - t_1) \quad (25)$$

The effect of changing G_R on the conversion-time curve can be shown if the effect of increasing polymer concentration on the overall rate of initiation is temporarily ignored. Using the G_R value of 0.69 and the calculated value of 0.40 the curves shown in figure 3.2 are obtained. Note that the theoretical curves are logarithmic while reported experimental curves are linear over the range shown.

The conversion-time data for the present work are reported in detail in section 5.1. The maximum percent conversion attained was approximately 65%, and up to that point the conversion-time curve is linear, confirming the data of Ballantine et al⁽³⁷⁾ and Landler⁽³⁸⁾. Discussion on the possible reasons for the differences between the theoretical and experimental curves is presented in section 6.1.

3.5 Molecular Weight Distribution

The reactivation of a dead polymer molecule into a growing

THEORETICAL CONVERSION
(POLYMER INITIATION IGNORED)

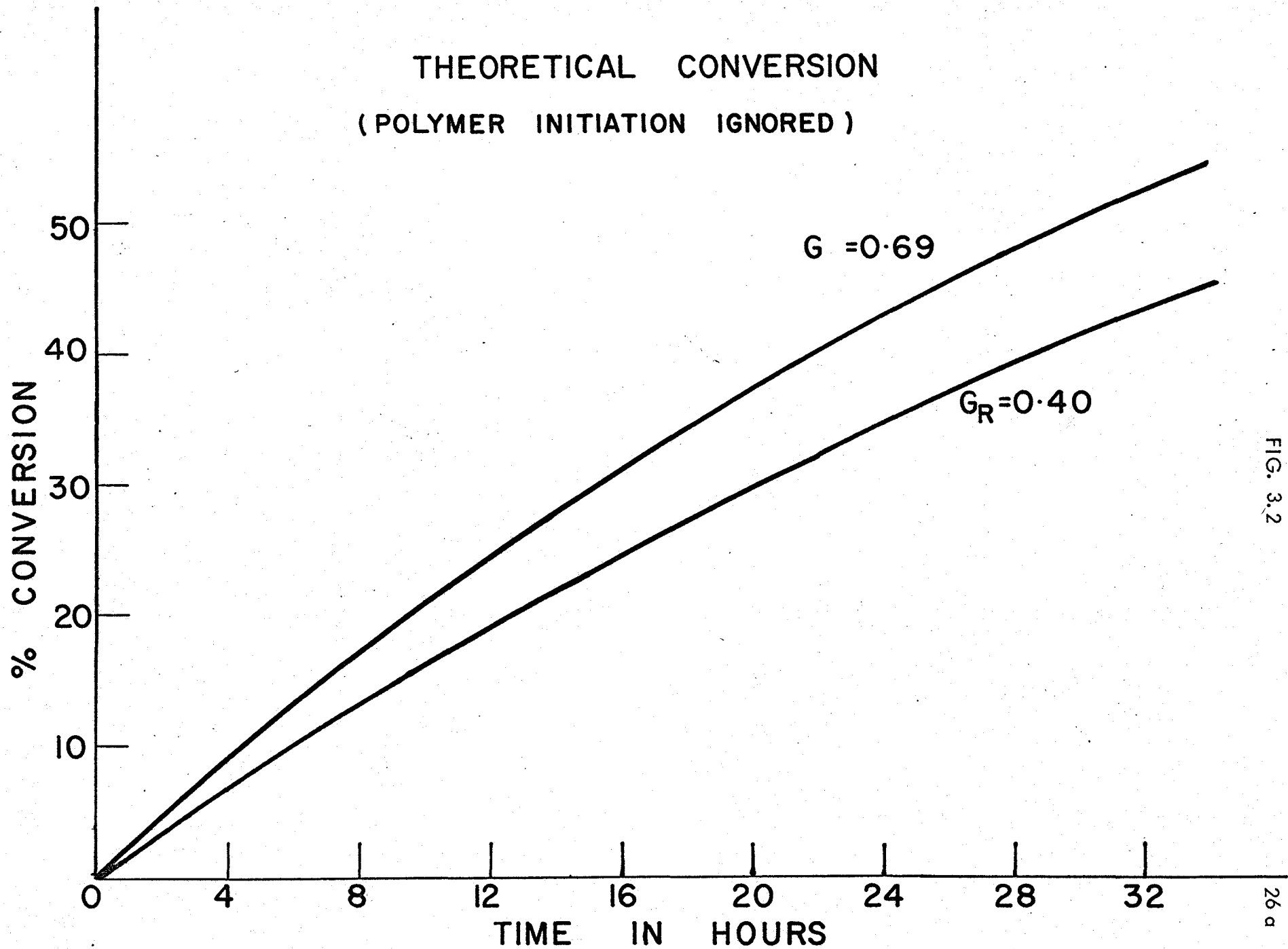
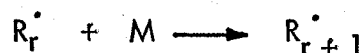


FIG. 3.2

chain will have a more significant effect on the molecular weight distribution than it will on conversion. If the G_R value of the polymer was twice that of the monomer, then at 50% conversion the rate of initiation would increase only one and one half times. However, if a dead polymer of chain length r is reactivated into a growing chain the resulting molecular weight of the polymer could be quite high. It is necessary, therefore, to introduce into the kinetic equations of catalysed polymerization the additional terms for polymer initiation. Since



and subsequently,



then the rate at which R_r^* is changing with time (i.e. $\frac{d[R_r^*]}{dt}$) in equation (3) will have the additional term; $k_{ip} [P_r]$, assuming k_{ip} is independent of polymer chain length.

For the bulk polymerization of styrene, $[S] = 0$ and $k_{td} = 0$, since there is no solvent present and termination by disproportionation is negligible. Applying the steady state assumption, the left hand sides of equations (2) and (3) become zero and the resulting equations are:

$$[R_1^*] = \frac{R_i + k_{fm} [M] [R^*]}{k_p [M] + k_{fm} [M] + k_{tc} [R^*]} \quad (26)$$

$$[R_r^*] = \frac{k_p [M] [R_{r-1}^*] + k_{ip} [P_r]}{k_p [M] + k_{fm} [M] + k_{tc} [R^*]} \quad (27)$$

Equation (4) will become

$$\frac{d[P_r]}{dt} = k_{fm} [M] [R_r^\cdot] + 1/2 k_{tc} \sum_{n=1}^{r-1} [R_n^\cdot] [R_{r-n}^\cdot] - k_{ip} [P_r] \quad (28)$$

The rate of initiation of monomer free radicals R_i , is given by equation (17) but for total rate of initiation including polymer molecules

equation (23) is used. From steady state considerations:

$$R_{it} = k_t [R^\cdot]^2 \quad (29)$$

and combining this with equation (23)

$$[R^\cdot] = \left[\frac{\{\phi_m [M] + \phi_p [P]\} I_R}{k_t} \right]^{1/2} = \left[\frac{\{G_R^m (MF) + G_R^p (PF)\} I_R}{1.095 \times 10^9 k_t} \right]^{1/2} \quad (30)$$

Where MF and PF are monomer weight fraction and polymer weight fraction respectively. This also assumes the same density for polymer and monomer.

Using the value of $[R^\cdot]$ from equation (30), equations (26), (27) and (28) can be solved consecutively for any given monomer concentration, that is at any given time t . The calculation of P_r permits the calculation of molecular weight averages which are:

Weight fraction of species r ;

$$W_r = \frac{r [P_r]}{M_o X} \quad (31)$$

the number average chain length;

$$\bar{r}_n = \frac{\sum_{r=1}^{\infty} r [P_r]}{\sum_{r=1}^{\infty} [P_r]} \quad (32)$$

and the weight average chain length

$$\bar{r}_w = \frac{\sum_{r=1}^{\infty} r^2 [P_r]}{\sum_{r=1}^{\infty} r [P_r]} = \frac{\sum_{r=1}^{\infty} r W_r}{W_r} \quad (33)$$

3.6 Influence of Viscosity

It has been pointed out in section 3.1 that Hui⁽²⁹⁾ found better agreement between experimental and theoretical results when k_t was corrected for viscosity changes. He found as might be expected, that the bulk viscosity of the system was a strong function of polymer weight fraction and also depended on the number average chain length. Relating the ratio k_t / k_{ti} to viscosity (where k_{ti} is the initial value of k_t), then permitted k_t to be calculated as a function of polymer weight fraction and number average chain length.

If the number average molecular weight of the polymer was relatively constant as a function of conversion as it was in this work (see Section 5), then viscosity corrections for changes in polymer weight fraction only would be required.

A plot of P_r vs. r , where r is the number of monomer units in the polymer chain gives the "frequency" distribution which is a graphical representation of the molecular weight distribution. If the experimentally determined molecular weight distribution from GPC measurements compares favourably with the theoretical distribution, then the kinetics assumed for the reaction must be fairly appropriate.

In the solution of equation (25) to give a theoretical conversion time curve, variations in k_t were not taken into account. As just discussed, however, k_t can be corrected for viscosity and the conversion-time curve modified accordingly.

Vaughan⁽³⁹⁾ and Robertson⁽⁴⁰⁾ studied the effect of viscosity on the thermal and catalysed polymerization of styrene, respectively. The change in the rate constants were explained in terms of diffusion control with k_t being the most sensitive to viscosity changes and k_p and other rate constants not appreciably affected except at very high viscosities. If diffusion control of the reaction is significant it might be expected that agitation of the reaction mixture would influence both the rate of conversion of monomer to polymer and also the molecular weight distribution.

4. EXPERIMENTAL

For details of sample preparation and analysis see Appendix A.

4.1 Reactor

Glass vials of approximately 10 cc capacity and containing six to eight glass beads, were filled with styrene, degassed and sealed under vacuum. The vials were held in spring clips on a vertically reciprocating and rotating rod (Fig.A.2) and encircled by the radiation source⁽⁴¹⁾ which consisted of twelve pencils of Co^{60} . The entire assembly was enclosed in an air bath maintained at 50°C.

For a normal experimental run, the vials were clipped in place (maximum of four at one time), the radiation source positioned with remote handling slave manipulators, and the agitator started. At predetermined time intervals the Co^{60} source was temporarily retracted while the vials were exchanged and then the process was restarted. Approximately five minutes were required to complete an exchange of vials.

The vials were opened, rinsed out with dioxane, and the contents slowly added to a tenfold excess of methanol. The precipitated polymer was filtered through fine pour fritted glass crucibles, dried under vacuum and weighed. Since each vial contained a known amount of styrene initially, the percent conversion to polymer was determined.

Similar experiments were carried out without agitating the samples to see if any differences in conversion or molecular weight distribution

could be attributed to agitation.

4.2 Analysis

4.2.1 GPC

Most of the agitated and non agitated samples were analysed by gel permeation chromatography. The data were read directly from the chromatograph in digital form and processed on the IBM 7040 computer (see Appendix A. 5). Peak elution heights for each sample were obtained to the nearest 0.05 of an elution count and \bar{M}_n , \bar{M}_w , and \bar{M}_z were found using Tung's Hermite polynomial method to correct for imperfect resolution⁽⁴²⁾.

4.2.2 Osmometry

Selected samples at 6, 12, and 18 hours irradiation time were analysed on a Hewlett-Packard membrane osmometer to obtain number average molecular weights, \bar{M}_n . Agitated and non-agitated samples were compared.

4.2.3 Intrinsic Viscosity

The samples analysed on the osmometer were also measured with a modified Ubbelohde viscometer to obtain intrinsic viscosity. In addition, a 2 hr. and 30 hr. sample were measured. Intrinsic viscosities were obtained in tetrahydrofuran at 30°C since this was the solvent used in the GPC.

4.2.4 Bulk Viscosity

Samples were prepared as in section 4.1 and irradiated,

without agitation, from 2 to 26 hrs. These samples were transferred directly to a constant temperature bath at 50°C and viscosities were measured with a Brookfield viscometer using a 0-500 cps spindle and a small sample holder.

5. EXPERIMENTAL RESULTS

5.1 Conversion - Time Data

The data for the percent conversion of styrene to polystyrene as a function of time are shown in tables 5.1 and 5.2. These data have been corrected for thermal polymerization by assuming a value of 0.025 percent per hour for the thermal polymerization rate at 50°C. (see figure 5.1).

The conversion - time data are represented graphically in figure 5.2. The agitated data and non-agitated data were regressed separately and both fitted to straight line equations. The dotted line in figure 5.2 above 28% conversion shows a probable trend in the data although insufficient data are available to make a definite conclusion.

The agitated and non-agitated data were tested to determine if there is any significant difference between them. The slopes of the two "best fit" straight lines were compared as described in reference (55) and the difference is not significant. When the data points are paired between agitated and non-agitated samples and tested to determine if the differences between them are significant, i. e., if the mean of the differences is significantly different from zero, the hypothesis that the mean is equal to zero is rejected at the 98% confidence level but accepted at the 99% level. Therefore, if the confidence limits on the plotted data are expanded to the 99% level, the agitated and non-agitated data can be represented by the same linear equation.

TABLE 5.1

Irradiation Time - Conversion Data
for Agitated Samples (50°C)

<u>Sample Code</u>	<u>Hours of Irradiation</u>	<u>% Conversion</u>	<u>% Conversion per hour</u>
1720	1	1.74	1.74
2720	2	3.64	1.82
3720	3	4.68	1.59
4720	4	6.46	1.62
4802	4	6.91	1.73
6720	6	11.49	1.92
8720	8	14.62	1.82
8729	8	14.60	1.82
10729	10	18.05	1.81
12729	12	20.95	1.75
14729	14	24.45	1.75
16729	16	27.30	1.71
18909	18	32.00	1.78
20909	20	37.10	1.85
22729	22.5	39.85	1.78
26909 (1)	26	51.10	1.96
26909 (2)	26	51.00	1.96

Avg. 1.79

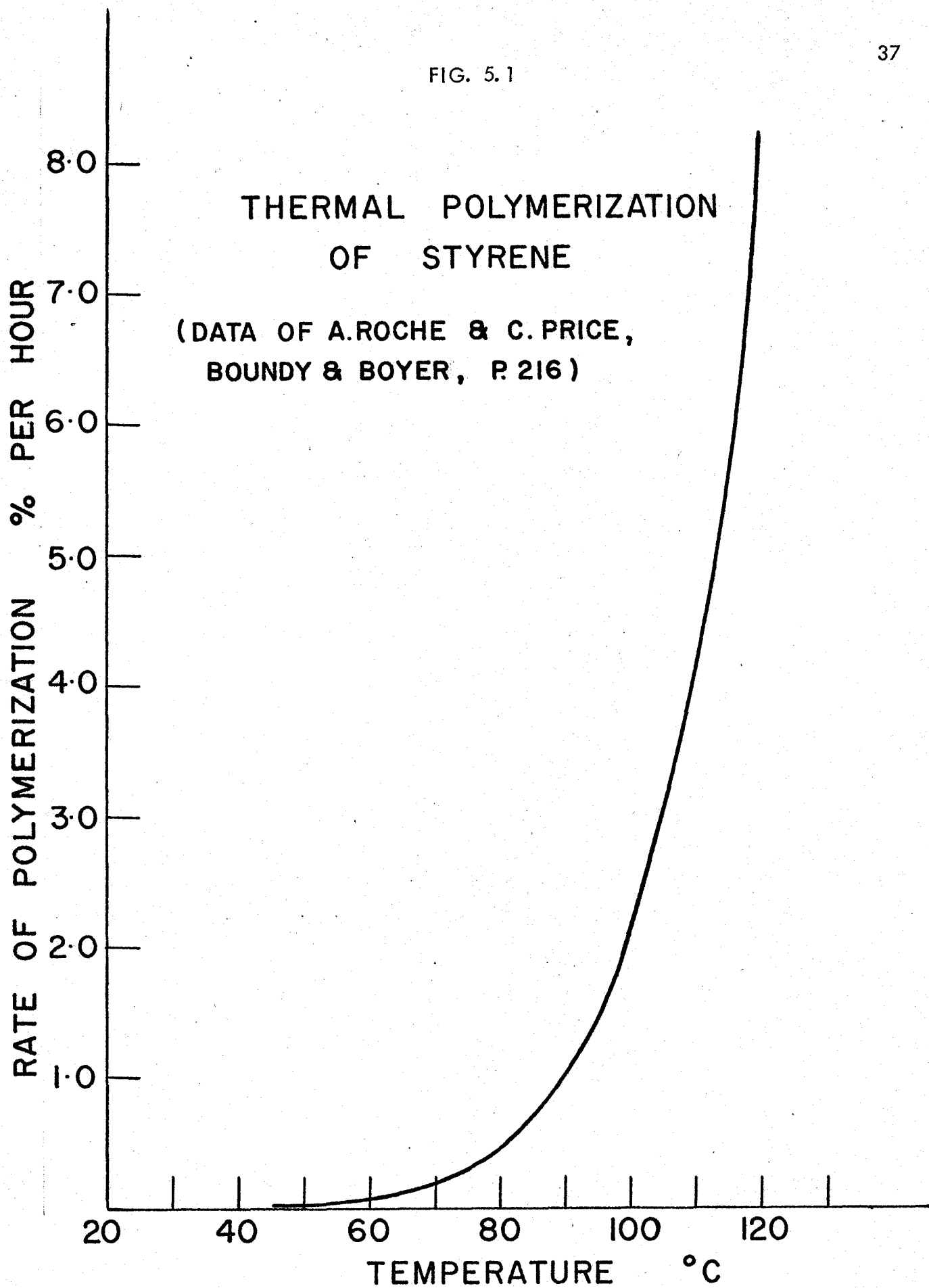
TABLE 5.2

Irradiation Time - Conversion Data

<u>Sample Code</u>	for Non-agitated samples (50°C)		<u>% Conversion per hour</u>
	<u>Hours of Irradiation</u>	<u>% Conversion</u>	
2822	2	3.30	1.65
4822	4	6.86	1.72
6822	6	9.65	1.61
8823	8	14.35	1.79
12824	12	19.60	1.63
14802	14.25	24.20	1.70
16802	16	26.30	1.64
18824	18	28.95	1.61
20808	20	35.05	1.75
22829	22	39.40	1.79
24823	24	41.10	1.71
26825	26	46.35	1.78
26808	26	57.45	*
30829 (1)	30	52.35	1.74
30829 (2)	30	54.35	1.80
30829 (3)	30	58.35	*
37808	37	67.87	1.83
			Avg. 1.77

*Precipitates formed were sticky and amorphous and difficult to dry properly.

FIG. 5.1



% CONVERSION VS TIME

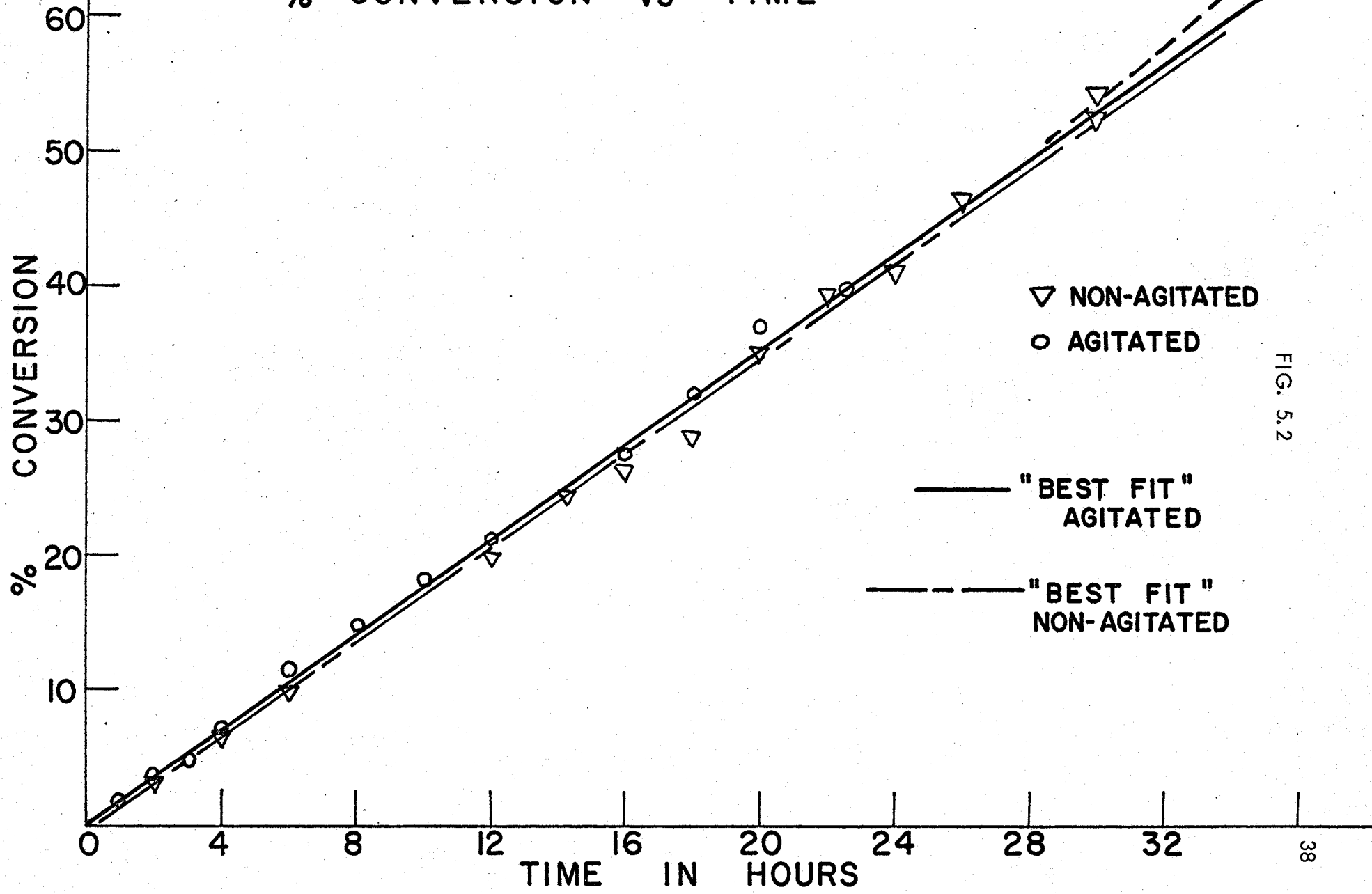


FIG. 5.2

Accepting these conditions, all of the conversion - time data were taken together and regressed to the straight line shown in figure 5.3. Also shown in figure 5.3 are theoretical conversion curves calculated from the equations discussed in appendix C.

Adjustments in the viscosity correction for k_t were made in the theoretical conversion equation to get the best possible fit to the experimental data. This theoretical curve is shown in figure 5.4 with all of the experimental conversion data agitated and non-agitated grouped together.

5.2 Viscosity Measurements

The bulk viscosity of the monomer - polymer mixture was measured at 50°C using the Brookfield viscometer as described in appendix A. A bulk viscosity vs. irradiation time graph is shown in figure 5.5. The same data plotted against polymer weight fraction, are shown on a semi-log plot in figure 5.6, from which the correlating equation given below was taken.

$$\ln \mu = 0.694 + 12.66 (\text{PF})$$

5.3 GPC Data

The results of the GPC analysis are shown in tables 5.3 and 5.4 for agitated and non-agitated samples respectively. The results were corrected for imperfect resolution using the method of Tung⁽⁴²⁾, referred to previously in section 4.2.1. All calculations are based on a linear sample calibration curve determined by plotting $\log M$ against elution counts.

EFFECT OF G_R^M AND G_R^P
ON THEORETICAL CONVERSION

% CONVERSION

80
70
60
50
40
30
20
10

0

4

8

12

16

20

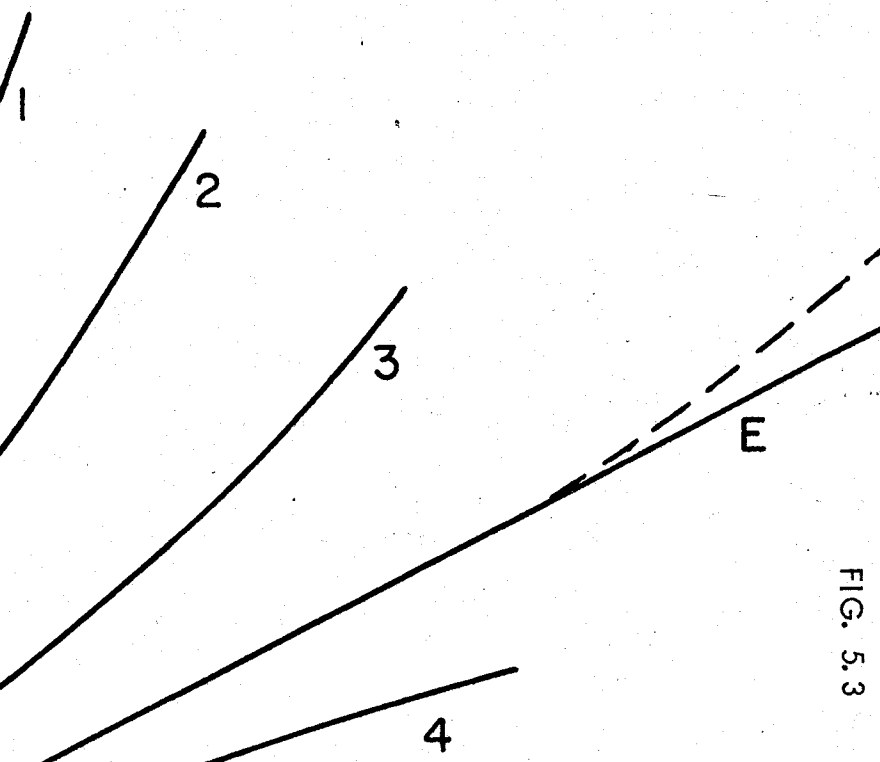
24

28

32

40

TIME IN HOURS



CURVE NO.	G_R^M	G_R^P	K_T
1	0.69	2.07	CORR. FOR μ
2	0.69	0.69	"
3	0.40	0.40	"
4	0.40	0.40	NO CORR. FOR μ
E	EXPERIMENTAL		FOR μ

FIG. 5.3

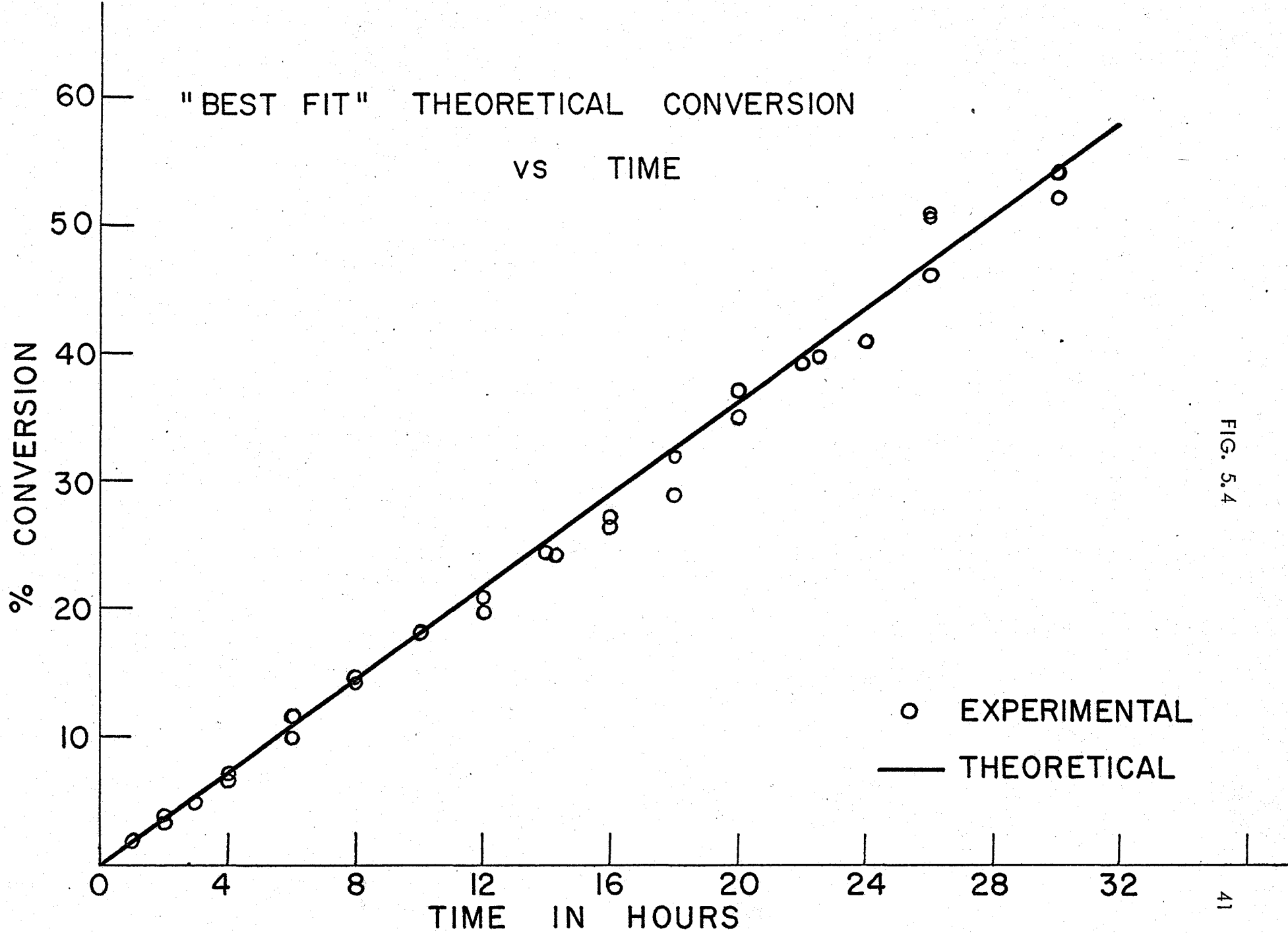
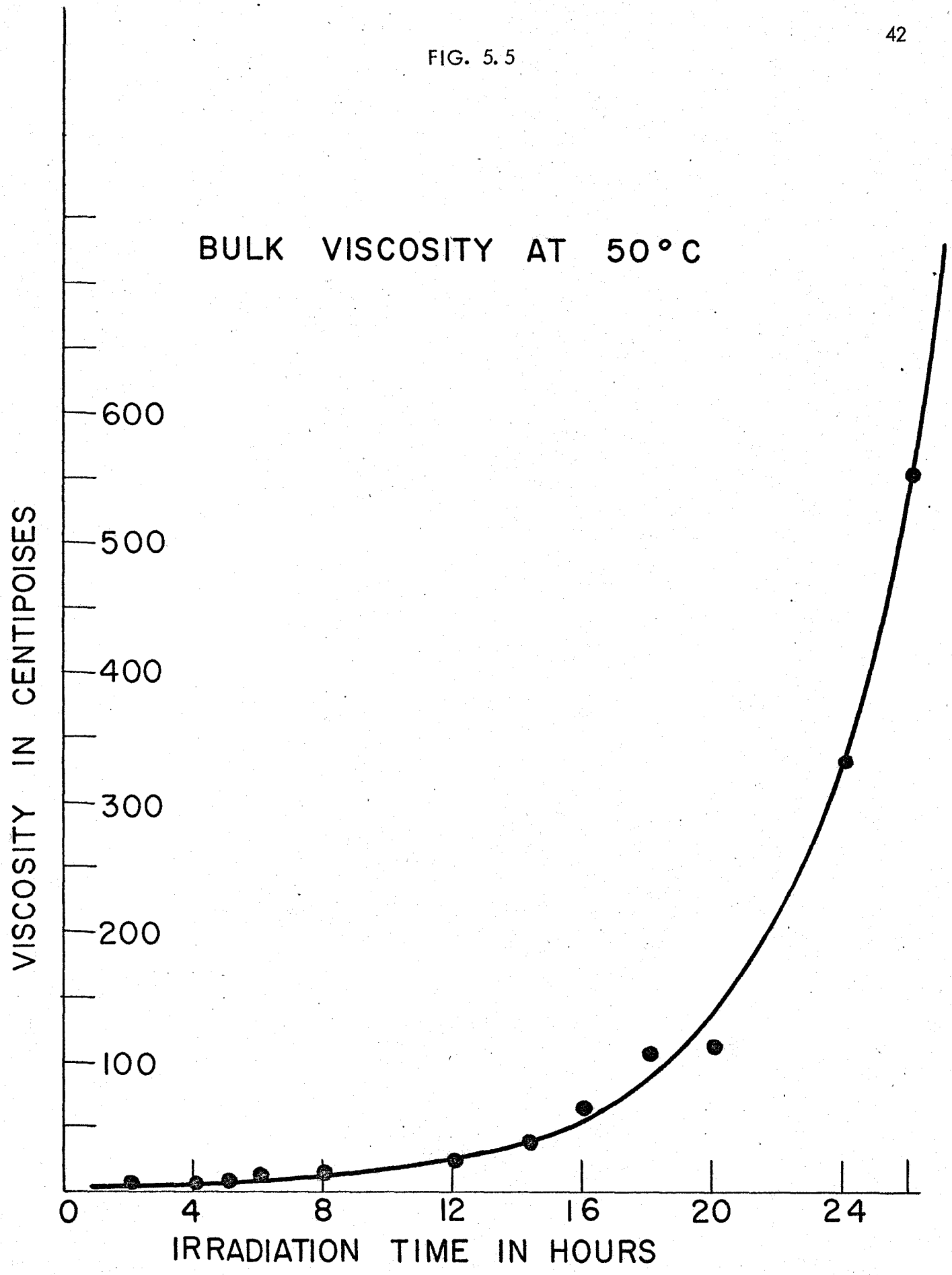


FIG. 5.4

FIG. 5.5

BULK VISCOSITY AT 50°C



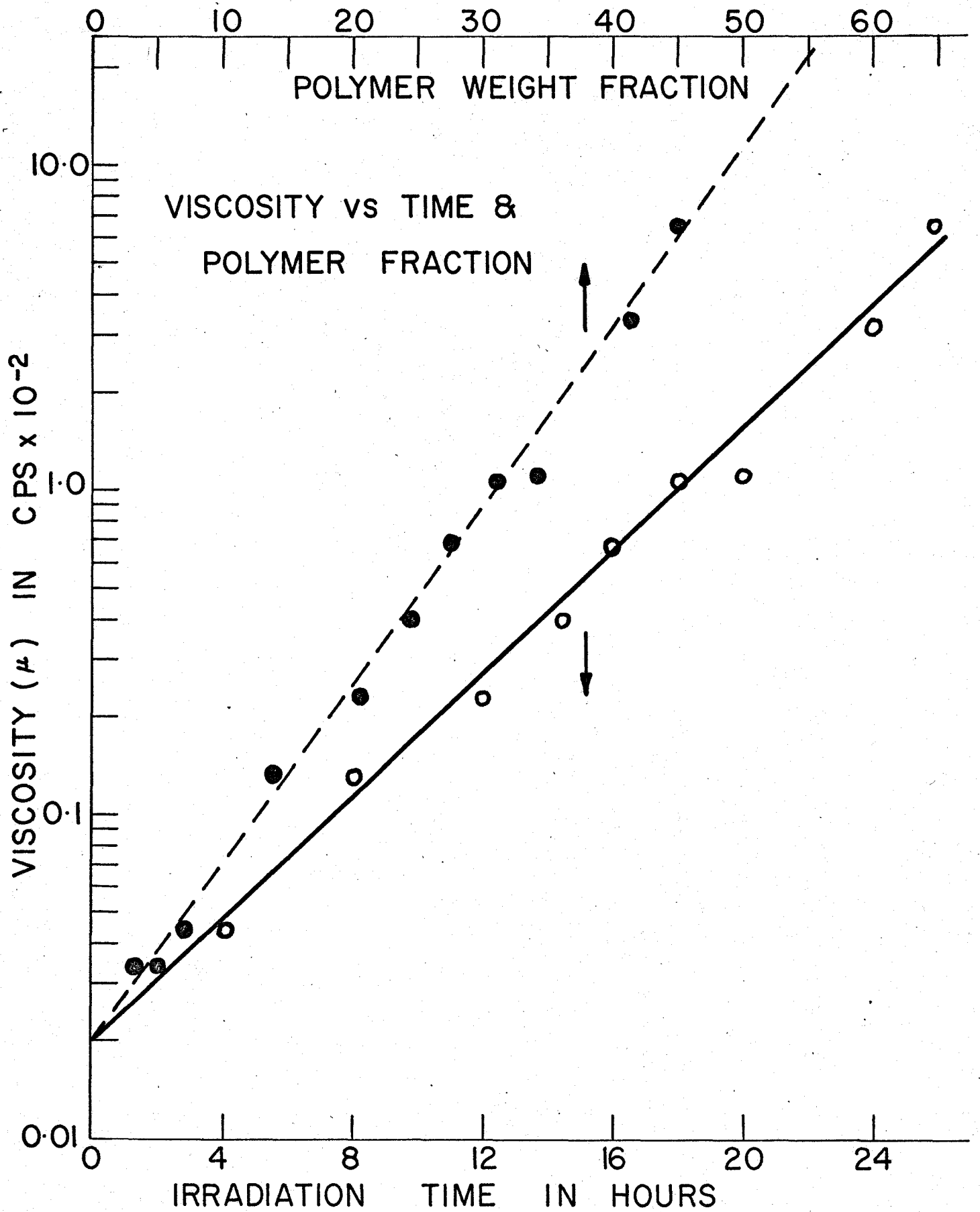


TABLE 5.3

GPC Data Agitated Samples

Sample Code	Irradiation Time (Hours)	\bar{M}_n	\bar{M}_w	\bar{M}_z	$\frac{\bar{M}_w}{\bar{M}_n}$
1720	1	26,200	45,400	69,300	1.731
2720	2	39,700	73,000	104,800	1.839
3720	3	38,800	73,800	110,400	1.904
4720	4	39,800	72,200	105,200	1.813
6720	6	39,000	69,200	100,800	1.771
8720	8	34,100	65,400	101,000	1.917
10720	10	32,600	61,700	94,800	1.891
12729	12	36,300	71,100	117,000	1.961
18909	18	35,300	65,600	95,700	1.860

TABLE 5.4

GPC Data Non-Agitated Samples

Sample Code	Irradiation Time (Hours)	\bar{M}_n	\bar{M}_w	\bar{M}_z	\bar{M}_w/\bar{M}_n
2822	2	43,400	70,200	99,700	1.617
4822	4	40,700	66,300	86,900	1.630
6822	6	46,400	74,300	101,200	1.602
8822	8	45,100	75,700	107,000	1.677
12824	12	38,500	67,300	98,600	1.747
18824	18	39,200	68,800	102,400	1.755
20808	20	36,600	61,000	82,500	1.667
22829	22	41,200	73,200	93,300	1.774
24823	24	43,900	74,900	115,300	1.706
26825	26	40,900	71,700	107,800	1.751
30829 (1)	30	43,800	74,900	106,800	1.710
30829 (2)	30	41,000	72,200	107,400	1.761
30829 (3)	30	40,800	73,400	106,900	1.801

5.3.1 Universal Calibration Curve

From the GPC analysis and intrinsic viscosity measurement of four linear polystyrene samples a universal calibration curve was constructed as shown in figure 5.7. The standards used, with the corresponding values of intrinsic viscosity and peak elution volumes are shown in table 5.5.

TABLE 5.5

Standards for Universal Calibration Curve

<u>Standard Sample Code</u>	<u>Molecular Weight</u>	<u>$[\eta]$</u>	<u>GPC Peak Elution Volume</u>	<u>$[\eta]M$ $\times 10^{-7}$</u>	<u>Calculated \bar{M}_v *</u>
3 A	411,000	120	16.6	4.93	414,000
41984	171,000	63	17.9	1.08	165,000
4 a	97,200	40	19.0	0.389	87,500
7 a	51,000	27	20.0	0.138	48,600

* Using Mark-Houwink Equation given in appendix A

5.4 Intrinsic Viscosity

The intrinsic viscosity of four linear polystyrene standards and eight selected samples was determined as described in appendix A.5.2. The viscosity average molecular weight of these samples was calculated by assuming the polymer was linear and using the Mark - Houwink equation established in appendix A.5.2.1. The data are shown in table 5.6.

FIG. 5.7

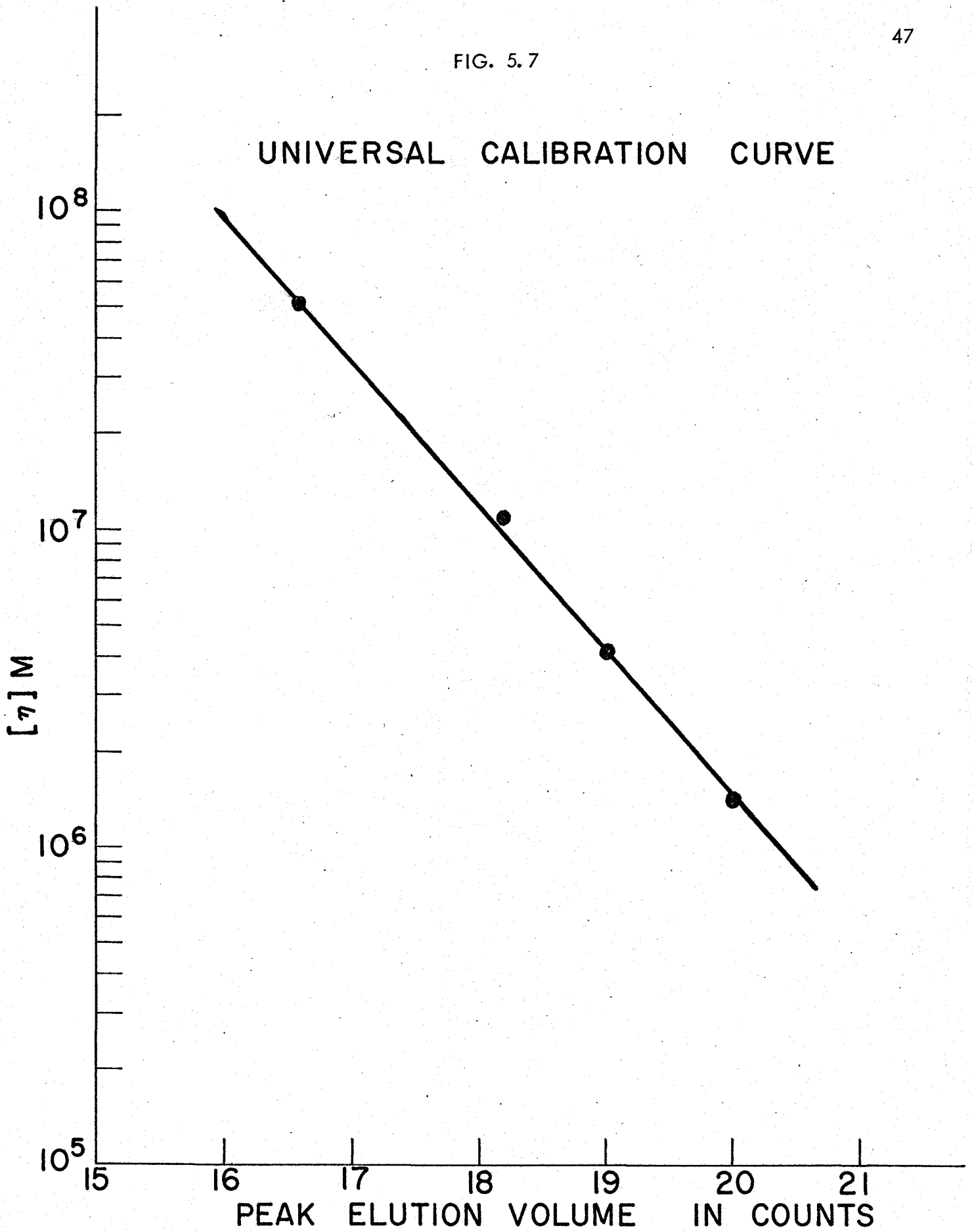


TABLE 5.6

Intrinsic Viscosities and Calculated Viscosity Average Mol. Wt.

<u>Sample Code</u>	<u>Irradiation Time (Hours)</u>	<u>Intrinsic Viscosity $[\eta]$</u>	<u>Calculated \bar{M}_v</u>	<u>Remarks</u>
2822	2	42.0	100,000	non-agitated
6822	6	46.0	108,000	"
12824	12	34.8	74,000	"
18824	18	32.0	64,000	"
30829	30	32.8	67,000	"
6720	6	39.5	90,000	agitated
12729	12	34.5	73,000	"
18909	18	36.8	82,000	"

5.5 Osmometry

The number average molecular weight for six selected samples was determined using a membrane osmometer as described in Appendix A. 5. 4. The value of \bar{M}_n obtained from the GPC is compared with \bar{M}_n from osmometry and M from the universal calibration curve in table 5. 7. The theoretical value of \bar{M}_n calculated by the program described in Appendix C, is also shown.

TABLE 5.7

Comparison of Molecular Weight Determinations

<u>Sample Code</u>	<u>Remarks</u>	<u>\bar{M}_n from GPC</u>	<u>\bar{M}_n from Osmometry</u>	<u>M from Universal Calibration Curve</u>	<u>Theoretical \bar{M}_n</u>
6822	non-agitated	46,400	45,100	50,000	58,000
12824	"	38,500	43,700	58,900	55,000
18824	"	39,200	46,100	54,700	53,000
6720	agitated	39,100	47,200	55,200	58,000
12729	"	36,300	45,300	59,400	55,000
18909	"	35,300	47,500	50,300	53,000

5.6 Molecular Weight Distribution

The weight fraction of each species r is defined by

$$W_r = \frac{r [P_r]}{M_0 X}$$

where M_0 is the initial monomer concentration and X is the fractional conversion of monomer to polymer. Figure 5.8 shows W_r as a function of r after approximately twenty five hours of irradiation. The experimental curve is based on the same GPC analysis from which the \bar{M}_n values listed in table 5.7 were taken.

WEIGHT FRACTION POLYMER
vs CHAIN LENGTH

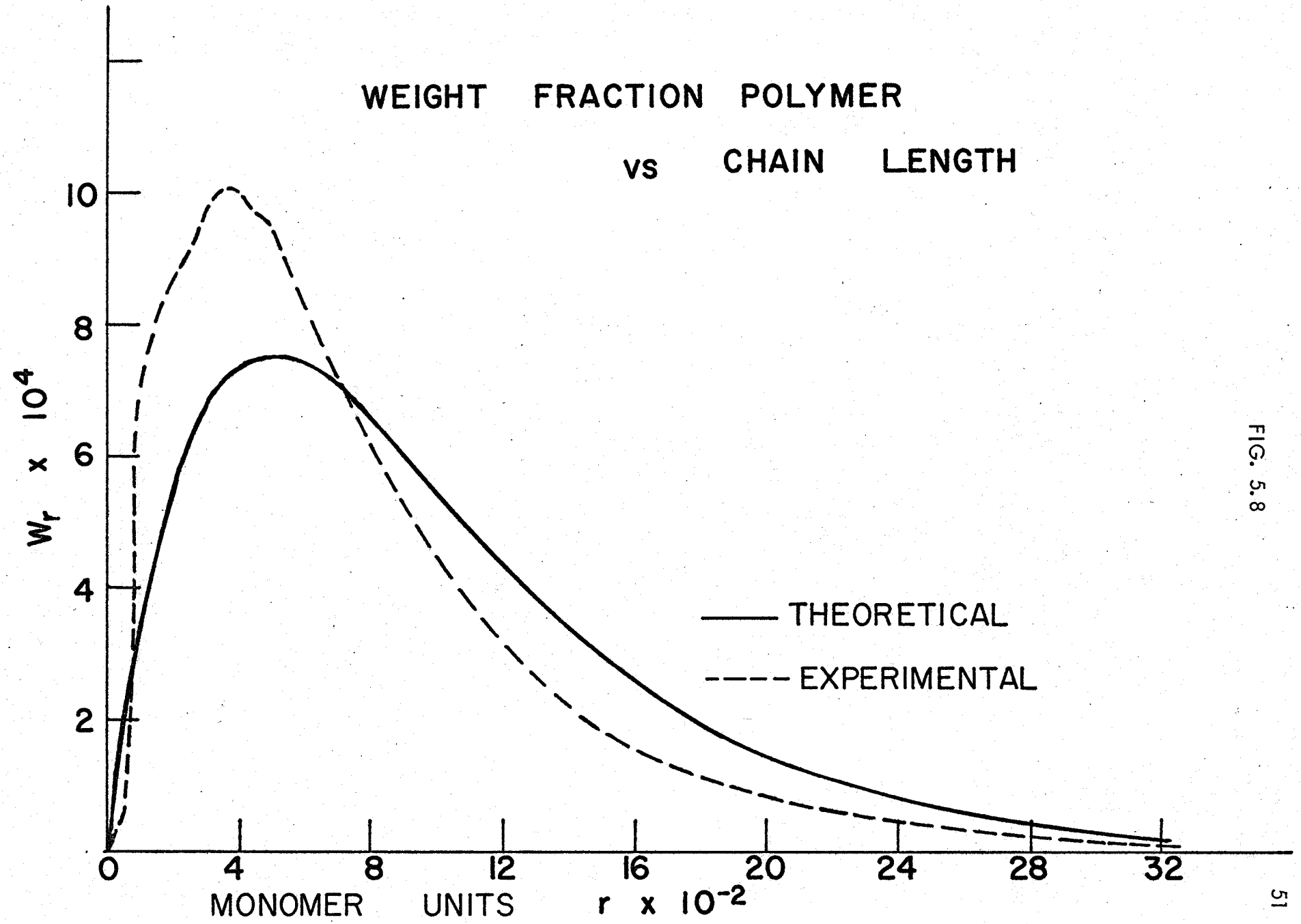


FIG. 5.8

6. DISCUSSION OF RESULTS

6.1 Conversion - Time Data

The regressed data giving percent conversion as a function of time showed that the percent conversion per hour is not affected by agitating the sample while it is being irradiated. This means that the kinetic equations and constants are unaffected by agitation of the system at least up to 50% conversion of monomer to polymer, i. e. when the viscosity is less than 1000 cps.

Although they have the same slope, whether or not the straight lines shown in figure 5.2 have the same intercept is not quite clear. If the confidence limits on the data are taken wide enough of course, all of the data will fit the same straight line, but if the lines are in fact different, only two explanations seem plausible. Shifting the conversion curve to the right on the graph would be consistent with a short induction period in the non-agitated samples although it is difficult to suggest any reason why the non-agitated samples should show an induction period which is not shown by the agitated samples. A more likely explanation is that a slight change in experimental techniques between the time the agitated and non-agitated samples were run resulted in a uniform but slightly different polymer yield.

At conversion above 50%, the high viscosity of the system made it difficult to obtain dry, monomer free, precipitates when the mixture was precipitated in methanol and vacuum dried. Consequently, the apparent increase in the slope of the experimental curve shown in figure 5.3 may or may not represent a real increase in the percent conversion per hour. Studying the percent conversion per hour data

in tables 5.1 and 5.2 also shows there is a very slight increase with time. If this effect is real the straight line plots of figure 5.2 are not justified and should in fact be slightly curved upward. However, the effect is very small and could be due to the difficulties experienced in handling viscous samples.

6.1.1 Theoretical Conversion - Time Curves

The theoretical curves shown in figure 5.3 illustrate the effect of three important parameters on the overall conversion. These are the G_R value for the monomer (G_R^m), the G_R value for the polymer (G_R^p), and the change in k_t with changes in viscosity. Curves one and two illustrate the lower conversion caused by a lowering of the G_R^p value. It is also obvious from these curves that the G_R^m value is too high to fit the experimental curve at any point. This is understandable, however, since the G_R^m value calculated for a conversion of 1.77% per hour was 0.40 as illustrated in section 3.3.1.

Although by definition of G_R (see section 3.3.1) the value of $G_R^m = 0.69$ may be valid, the important consideration from the standpoint of the reaction kinetics is not how many free radicals may be formed during a particular time but how many will actually propagate a chain and result in the formation of a polymer molecule. If, as Chapiro⁽³²⁾ suggests, at dose rates above 2 or 3 rads/sec there are more free radicals produced per unit time than can react with monomer and consequently they recombine without initiating polymer chains, then a limiting free radical concentration must exist. Above this limit, free radicals would recombine as quickly as

they are formed. There is some evidence⁽³³⁾ to suggest that this limiting free radical concentration is temperature dependent and that at higher temperatures more free radicals would propagate polymer chains than at lower temperatures. However, the evidence is very limited and it is not certain whether or not it is vitiated by the thermal polymerization of styrene at the higher temperature.

Since the G_R value discussed here is determined from the actual kinetics of polymer chain propagation which may or may not be related to the number of free radicals produced when the dose rate is above some critical value, then it would be more meaningful to define an "effective G_R value" as follows:

$$\text{Effective } G_R = \frac{\text{No. of free radicals initiating polymer chains}}{100 \text{ e. v. absorbed}}$$

By this definition, the effective G_R^m would be 0.40 at 50°C.

If the concentration of free radicals which will actively result in the consuming of monomer molecules has a maximum limit, then this limit would also apply to free radicals generated in the polymer, irrespective of the fact that the polymer molecule is more likely to form a free radical than is a monomer molecule. For this reason, the experimental G value of 0.40 would also apply to the polymer giving an effective $G_R^p = 0.40$ at 50°C.

The theoretical conversion (curve no. 3) shown in figure 5.3 is based upon G_R^m and G_R^p both equal to 0.40 and is in good agreement with the experimental curve up to 10% conversion.

The effect of modifying k_t as a function of viscosity is illustrated in figure 5.3 (curve no. 4). Curves no. 3 and no. 4 are the same except that no corrections have been made for k_t in curve no. 4. Since the experimental curve lies between no. 3 and no. 4, it suggests that a proper choice of the function relating k_t and viscosity would provide good agreement between the theoretical and experimental curves. This agreement (illustrated in figure 5.4) has been obtained by using the k_t - viscosity equation

$$\log k_t/k_{ti} = -0.133 \log (1 + \mu) - 0.025 (\log (1 + \mu))^2$$

and shows that the conversion - time data can be predicted up to 50% conversion in the bulk styrene system.

Small changes in dose-rate (up to 5%) do not appreciably change the conversion curves. This permits some flexibility in the experimental determination of this quantity and justifies the choice of an average dose-rate as determined in appendix B.2.1.

From equation (25) giving conversion as a function of time it can be seen that conversion depends upon the product of G_R and dose - rate. If the assumption of a limiting free radical concentration is true, then increasing the dose-rate should not give higher conversions. It would also follow that if the dose-rate is increased, the effective G_R value would decrease keeping the product of G_R and dose-rate relatively constant. This provides a method of checking the assumption, since as long as the dose-rate is above the "critical value" increasing it or decreasing it would

not change the conversion-time relationship if the temperature was kept constant.

6.2 Viscosity Measurements

The bulk viscosity data plotted in figure 5.5 were obtained from samples prepared in the same manner as those used for determining percent conversion. Consequently, for each sample irradiated it was possible to determine the corresponding conversion from figure 5.2 and plot the viscosity vs. polymer weight fraction curve in figure 5.6.

Although the range of viscosity measured in this case permitted extrapolation to the maximum conversion obtained, measurements at higher conversions would be necessary if the viscosity - polymer fraction correlations were to be extended much above 50% conversion. This would require the measurement of viscosities above 1000 cps. which was not possible with the Brookfield viscometer used in this work.

6.3 GPC Data

The reproducibility of molecular weight distributions as measured by the GPC is illustrated by the 30 hour irradiation time samples in table 5.4. A spread of about 3000 in number average molecular weight was observed.

A comparison of the number average molecular weight for agitated and non-agitated samples shows that the values for the agitated samples are slightly below those of the non-agitated samples. There does not appear to be much difference however, between the weight average molecular weights. Consequently the ratio of \bar{M}_w / \bar{M}_n for the agitated samples is somewhat higher than that for the non-agitated

material.

If these are real differences it would be consistent with the condition that the agitated material was more highly branched or cross linked than the non-agitated material, since the GPC would treat branched polymers as lower molecular weight linear polymers. There are, however, several other factors that could influence the \bar{M}_n and \bar{M}_w values calculated from the GPC analysis. These could include skewing of the chromatogram due possibly to viscosity effects, and differences in the polydispersity of the samples. Furthermore, it is not known if the GPC would treat branching in a consistent manner or if the results from branched material would be reproducible.

Within this framework of unknown factors it is not possible to make any definite statements about the effect of agitation on the molecular weight distribution of the polymer. It is fairly certain, however, that \bar{M}_n and \bar{M}_w are relatively constant over the entire polymerization period; an observation which is consistent with that of Ballentine et al ⁽³⁷⁾.

6.4 Universal Calibration Curve

The universal calibration curve of figure 5.7 together with the intrinsic viscosity measurements given in table 5.6 and peak elution volumes determined by the GPC, was used to give the value of M for several samples listed in table 5.7. Since this M is based on a curve made with monodispersed standards, whether it is \bar{M}_n , \bar{M}_w , or \bar{M}_v is not known, but likely it is some combination of all three. This would give values of M slightly greater than those for \bar{M}_n which is the basis of comparison in table 5.7.

The universal calibration curve is very sensitive to changes in peak elution volume. Because of this, even a slight error in determining the true position of the graph or the peak elution volume will result in large changes for M . For example, a difference in peak elution volume of 0.1 for a sample with an intrinsic viscosity measurement of 40, would result in a difference of 10% in the value of M .

6.5 Osmometry

The values of molecular weight determined by the membrane osmometer are based on sample concentration in weight percent and the number of solute molecules in the system. The molecular weight found in this way is the number average value, \bar{M}_n and is independent of the shape of the solute molecule provided it is large enough not to pass through the semi-permeable membrane. Osmometry, therefore, provides the best measure of absolute number average molecular weight.

6.6 Molecular Weight Distribution

The theoretical molecular weight distribution curve after approximately 25 hours of irradiation is shown in figure 5.8 and is typical of the distribution curve obtained at other time periods. When conversions are low, i. e. at short irradiation times, the peak value of W_r occurs at a chain length of about 600 monomer units and the weight fraction of high molecular weight material is still significant at a chain length of 3000 monomer units. For longer irradiation times, the peak value of W_r moves to the left and W_r for r equal to 3000 decreases slightly causing a decrease in both \bar{M}_n and \bar{M}_w with time. Since \bar{M}_n and \bar{M}_w will be in error when the contribution from the high molecular weight tail is still significant, the best value for both averages is obtained at a reaction time in excess of 25 hours.

Although the theoretical values of \bar{M}_n are shown in table 5.7 corresponding to different reaction times, these values are more in error at six hours than at eighteen hours. The value of \bar{M}_n calculated after 27 hours of irradiation is 50,700.

The experimental curve in figure 5.8 shows a higher percentage of low molecular weight material than the theoretical curve. This is consistent with the expected behaviour of branched or cross linked material in the GPC which would usually have a smaller hydrodynamic volume than linear material of the same molecular weight and would elute at a time corresponding to lower molecular weight material. This would cause the weight fraction of low molecular weight material to appear higher than it actually is.

7. CONCLUSIONS AND RECOMMENDATIONS

7.1 Conclusions

The polymerization of styrene saturated with water (500 ppm), at 50°C, and initiated by gamma radiation, occurs by a free radical mechanism. The rate of initiation of the system can be expressed in terms of the G value of radical production in both monomer and polymer.

If a kinetic mechanism is assumed in order to calculate an "effective G_R " for monomer and polymer, then a simple kinetic model can be used to predict conversion up to about 50% in a bulk system, provided the termination constant k_t is corrected for changes in the viscosity of the polymerizing medium.

Although the theoretical model developed in this study will predict conversion and molecular weight distributions, the experimental methods used for measuring MWD were not sufficiently accurate to determine if the theoretical calculations were completely valid. However, deviations between theory and experiment occur in a predictable manner suggesting that the theoretical equations are correct.

The effect of agitation on conversion and MWD is indefinite. Small differences observed between agitated and non-agitated samples could be due to experimental uncertainties although the possibility that the differences are real cannot be eliminated.

Polymer formed by radiation initiation is branched and/or crosslinked, even after very short irradiation periods. Although no accurate methods of measuring branching were available, irradiated samples did not behave similar to linear polymer in the GPC or during viscosity measurements.

7.2 Recommendations

The use of the classical equation relating reaction rate to the square root of initiation was possible when an "effective G_R " was used and it was assumed that at high initiation rates many free radicals recombined without initiating polymer chains. This implies that at a given temperature, a limiting free radical concentration exists and faster polymer chain initiation rates are not possible. This assumption should be investigated by studying bulk polymerization at dose-rates above, and below the one used in this work.

Extending the present study to conversions of 90% or more would test the validity of the kinetic assumptions at viscosities above 1000 centipoises. The expected sharp increase in the slope of the conversion vs time curve above 60% conversion might be accounted for by considering both k_t and k_p as functions of viscosity and/or polymer chain length.

An accurate method of measuring MWD is essential before the theoretical equations can be verified. Methods of treating branched or crosslinked material on the GPC should be fully investigated to determine if branching can be predicted satisfactorily. In addition, osmometry and light scattering techniques should be employed to permit independent measurements of \bar{M}_n and \bar{M}_w .

A study of branching and crosslinking, and possible degradation in polystyrene should be pursued when an accurate method of measuring these parameters has been found. Although generally considered to be a non-degrading polymer under irradiation it is possible that both branching and degradation occur but at different rates.

APPENDIX A

EXPERIMENTAL DETAILS

A. 1 Sample Preparation

All polymerization reactions were carried out in 10 c. c. hard glass annealed vials. The vials had a constricting neck ending in a standard male tapered joint as shown in figure A. 1. Six to eight 5 mm glass beads were added to each vial before the neck and taper joint were fitted and in four samples stainless steel beads were used instead of glass.

A 10 cc hypodermic syringe was used to fill and empty the vials since the neck was too narrow to permit free liquid flow. The syringe was fitted with a 19 gauge , 3 inch stainless steel needle with a "Luer-lok" connection.

Regular laboratory glassware detergent was used to clean the vials. The detergent solution was injected and removed with the syringe and the vials rinsed approximately ten times with distilled water and once with methanol. They were then dried in the oven for about one hour.

The reaction vials were filled with 10 cc aliquot samples of styrene. (See table A. 1 for an analysis of the styrene used). Necessary precautions were taken to ensure that the styrene was injected below the constriction in the neck of the vial and that air was not entrapped in the sample during this process. Several checks on the delivery accuracy of the syringe gave a sample weight of 8.808 \pm 0.026 grams or a maximum variation of approximately 0.3 percent.

FIG. A.1

GLASS REACTION VIAL

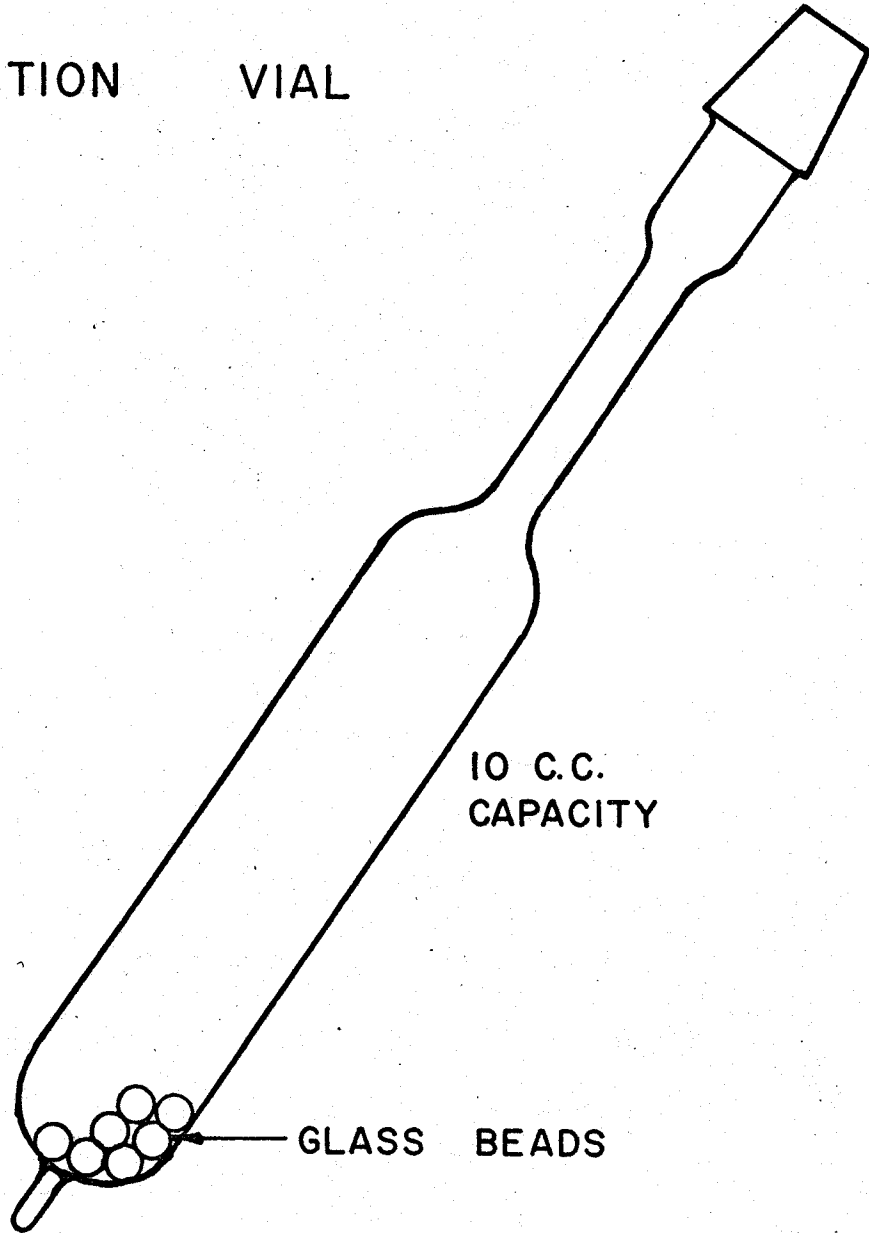


TABLE A. 1

STYRENE ANALYSIS

<u>Name</u>	<u>Weight Percent</u>
Styrene	99.630
Ethyl benzene	0.032
Isopropyl benzene	0.123
N-propyl benzene	0.090
Sec-butyl benzene	0.039
α - methyl styrene	0.037
Sulphur	0.0004
Chlorides	0.0001
Benzaldehyde	0.0033
Peroxides (H_2O_2)	0.0012
Polymer	0.0016
Water	Saturated 500 ppm.

This styrene was supplied courtesy of K. Tebbens, Polymer Corporation.

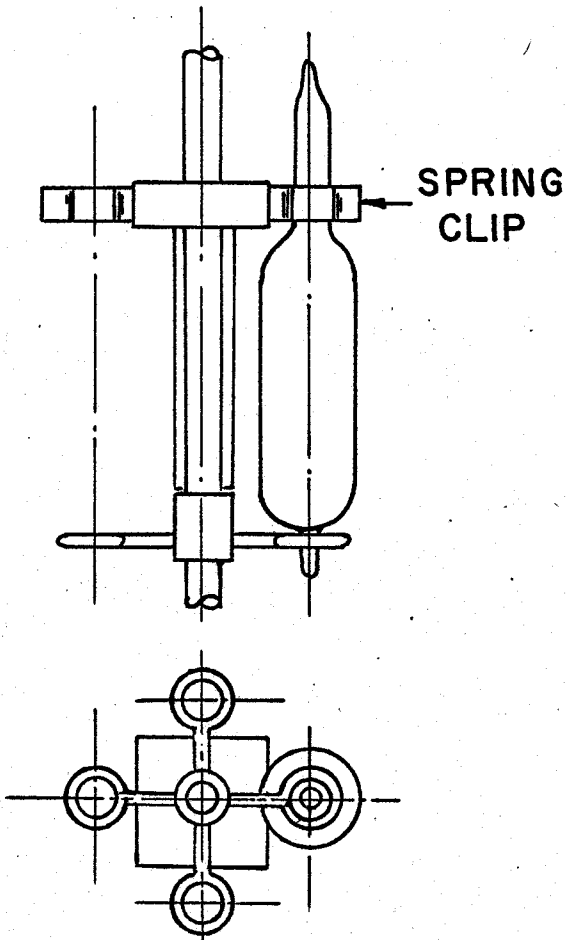
This is slightly less than 10 c. c. of styrene. When filled, the vials were stoppered and stored in the refrigerator while awaiting the degassing operation.

Before irradiating the samples it is essential that all traces of oxygen be removed from the system since oxygen acts as a radical scavenger and causes erratic results if present during polymerization. The vacuum system available for degassing permitted three samples to be handled at the same time. With the vials fitted onto the vacuum line the samples were frozen in liquid nitrogen and allowed to stand for fifteen minutes before evacuation. Each sample was held for at least one hour under a vacuum of better than 10^{-6} mm of mercury before it was sealed and removed. The vials were sealed by fusing the glass at the thin neck below the taper joint while still under vacuum. Since subsequent polymerization of the samples gave reproducible results and no induction periods were observed, this degassing procedure was considered adequate. The sealed samples were stored in the refrigerator prior to irradiation.

A.2 Sample Irradiation

The sample holder and agitator are shown in figure A.2. The centre rod moves vertically with a half inch oscillation at approximately one hundred to one hundred and fifty strokes per minute, and rotates, slowly when the cam is slightly off centre. In operation the glass or stainless steel beads are thrown up and down thus providing agitation in the styrene-polymer mixture. Agitation was judged effective up to about thirty percent conversion of styrene to polymer, at which point the viscous medium impedes the stirring action. A speed reducer on the cam

SAMPLE HOLDER



SAMPLE AGITATOR
& AIR BATH

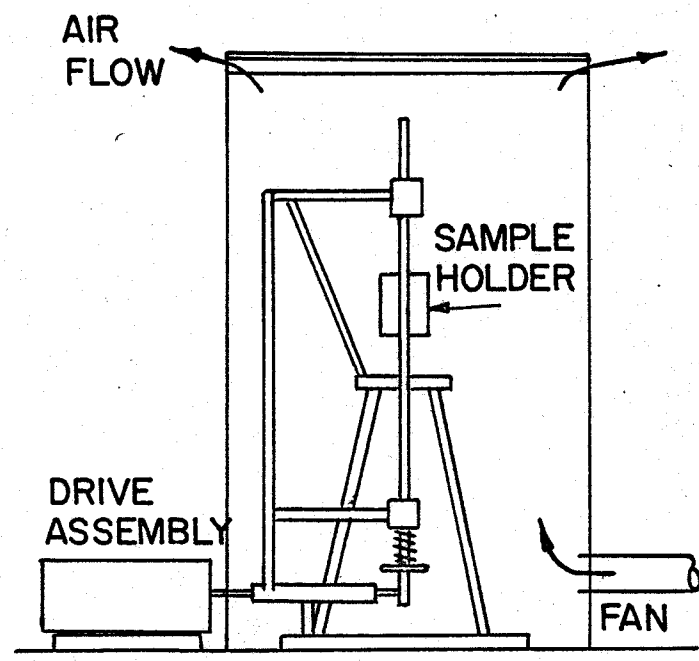


FIG. A.2

shaft allowed the agitation to be controlled from zero to the maximum of about one hundred and fifty strokes per minute. The entire unit except for the motor and speed reducer was encased in an air bath consisting of a plywood box with lid into which air was blown continuously. Two 750 watt heaters were located in the air duct where it entered the box. One heater was connected directly to the line voltage of 110 volts while the other was connected through a relay operated by a DeKhotinsky thermoregulator set for 50°C. Two thermocouple probes located within a few inches of the samples provided continuous temperature monitoring. Since the design of the system required that the heaters be shut off when samples were being added or removed from the shaker the temperature at the beginning of each run was less than 50°C and approximately ten minutes were required to bring it up to 50°C. Once the required temperature was attained control was within plus or minus 3°C.

With the samples in place within the shaker the Co^{60} source was brought into position with the remote handling devices. A complete description of the source is given in reference (41). When the source was in place the agitator and heaters were started. Agitated samples were irradiated from one to twenty six hours and non-agitated samples from two to thirty seven hours. The irradiation times for all samples are shown in tables 5.1 and 5.2.

When the irradiation time was completed the samples were removed immediately from the reactor and the percent conversion to polymer determined as described below.

A. 3 Determination of Conversion

The technique used for removing the monomer-polymer mixture from the reaction vials was in part dependent upon the extent of the conversion i. e. the viscosity of the mixture. For most samples, the neck of the vial was broken open and the mixture was forced into a 200 ml beaker containing about 20 ml of dioxane, by inserting the syringe, filled with air, part way into the inverted vial and slowly injecting the air into it. When most of the reaction mixture had been removed in this way the syringe was filled with dioxane and the vial was rinsed several times until all traces of the mixture were removed. The quantity of dioxane used was greater for viscous samples but in most cases was less than a total of 40 c. c. The dioxane-styrene-polystyrene mixture was stirred until it appeared that all of the polymer had dissolved in the dioxane. The solution was then added very slowly with vigorous stirring into 150 ml to 200 ml of methanol (at room temperature) in a 600 ml beaker⁽⁴⁷⁾. Although polystyrene is insoluble in methanol it is probable that the smallest polymer molecules such as the dimers and trimers would be soluble.

The precipitate formed was allowed to settle for at least twelve hours before it was filtered through a fine-pore sintered glass crucible. The precipitate was dried for a minimum of ten hours in a vacuum oven at about 70°C and then weighed. Subsequent redrying and reweighing of the precipitate showed no significant weight change indicating that the drying procedure was satisfactory. Percent conversions were determined using the initial sample weight of 8.808 grams.

A. 4 Bulk Viscosity Determinations

Samples were prepared as described in sections A. 1 and A. 2 and irradiated without agitation for from two to twenty six hours. Immediately after irradiation the samples were emptied into a Brookfield viscometer cup at 50°C and viscosity readings were taken using the Brookfield spindle No. S-SP-865A. The viscosity of the twenty six hour sample was slightly greater than 500 centipoises which was the upper viscosity limit for the spindle used. No other spindles were available to measure viscosities greater than 500 cps for samples of less than 10 cc total volume.

A. 5 Polymer Characterization

A. 5. 1 Gel Permeation Chromatography

A detailed discussion of the operation of the GPC and interpretation of the data can be found in references (1) and (48).

The samples for GPC analysis were prepared by making 10 ml of 0.05 weight percent solution of polystyrene in tetrahydrofuran (THF). The flow rate used was 3 ml/minute with a sample injection time of 20 seconds. The GPC output was obtained in graph form and also digitized on paper tape. The digitized data were processed by the IBM 7040 computer to provide input data for the Tung⁽⁴²⁾ correction program for imperfect resolution and also to provide intermediate values of elution volumes and heights by interpolation of the experimental values. A listing of the digital translator program used for this purpose is given in appendix D. The results of the Tung⁽⁴²⁾ program giving molecular

weight distributions and number and weight average molecular weights are given in section 5.

A. 5.2 Intrinsic Viscosity

The dynamic viscosity (η) of a fluid is the tangential force on unit area of either of two parallel planes at unit distance apart when the space between the planes is filled with the fluid and one of the planes moves relative to the other with unit velocity. In the c. g. s. system the unit of dynamic viscosity is the poise (one dyne second/cm²) and most liquids at room temperature have a viscosity of the order of one centipoise i. e. one-hundredth of a poise.

The proposal that there is a relation between the molecular weight of a polymeric solute and the viscosity of the polymer solution was first made by Staudinger ⁽⁴⁹⁾ in 1930. For most polymer-solvent systems this relation is not a simple one except at very low solute concentrations, hence most viscosity measurements are made at low concentrations and the results extrapolated to zero concentration. The viscosity obtained in this way is called the intrinsic viscosity or limiting viscosity number and is defined as:

$$[\eta] = \lim_{c \rightarrow 0} \left[\frac{\ln (\eta/\eta_0)}{c} \right] \text{ where } \eta_0 \text{ is the viscosity of the solvent.}$$

Onyon ⁽⁵⁰⁾ lists an alternate expression for $[\eta]$ together with other

viscosity terms and definitions.

The intrinsic viscosity can be related to the molecular weight of the polymer by the empirical equation:

$$[\eta] = K M^a$$

known as the Mark-Houwink equation (51) (52). Here K and a are constants for a given polymer, solvent, and temperature.

The molecular weight obtained by this equation is the viscosity average molecular weight \bar{M}_v defined theoretically by the relationship:

$$\bar{M}_v = \left[\frac{\sum N_i M_i^{1+a}}{\sum N_i M_i} \right]^{1/a}$$

This value will fall between the number average and weight average molecular weights, hence for a monodisperse sample the three molecular weights would be the same. In a polydisperse system \bar{M}_v will always be closer to \bar{M}_w than it will to \bar{M}_n .

The Mark-Houwink constants are generally obtained using monodisperse linear polymers of well defined molecular weight. It would be expected, therefore, that polydisperse, branched polymers would show considerable deviation from the Mark-Houwink equation. For a given \bar{M}_n a polydisperse polymer will always have a higher intrinsic viscosity than a monodisperse material, irrespective of the nature of the molecular weight distribution⁽⁵³⁾. The effect of branching on intrinsic viscosity has been studied⁽⁵⁴⁾ although the results are not perfectly clear due to possible inefficient fractionation of the polymer and consequent broadening of the

molecular weight distribution.

A. 5.2.1 Experimental

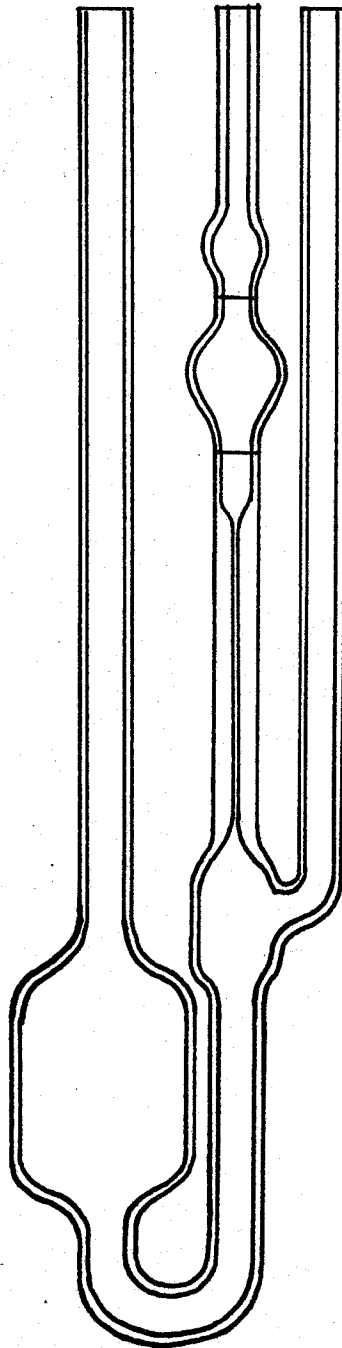
Since the determination of intrinsic viscosity requires only the ratio of dynamic viscosity measurements, it is not necessary to determine viscosities in absolute units such as centipoise. Measurements are conveniently made using a modified Ubbelohde dilution viscometer shown in figure A. 3, a constant temperature bath with control to at least $\pm 0.02^\circ\text{C}$, and a stopwatch. The most important factor is to be sure the viscometer is very clean and that normal precautions are observed to keep dust or foreign particles out of the solutions when viscosities are to be measured.

Four of the linear polystyrene standards used to calibrate the GPC were chosen to determine the Mark-Houwink constants for the polystyrene - THF system. A solution of concentration 0.003 gram/ml was prepared by weighing the standard sample into a 50 ml volumetric flask, placing it in a constant temperature bath at 20°C (the calibration temperature) and filling to the mark with THF which had been filtered twice. Additional solutions of 0.0015 gm/ml and 0.00075 gm/ml were prepared by diluting the original solution as required.

The viscometer was cleaned several times with cleaning solution, thoroughly rinsed with distilled water, then methanol,

FIG. A.3

UBBELOHDE DILUTION VISCOMETER

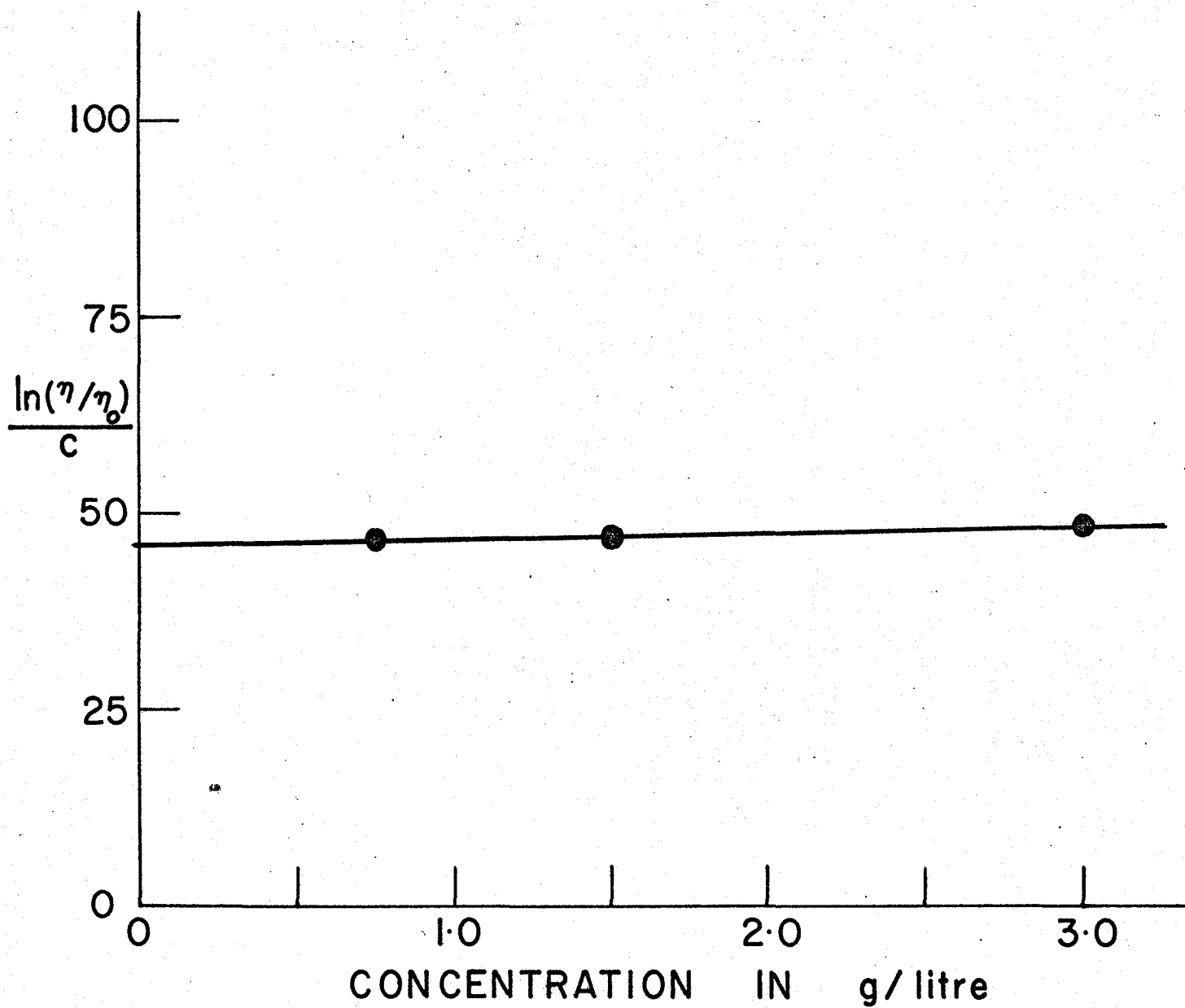


and dried in the oven. When dried it was rinsed twice with filtered THF then filled with approximately 10 cc of THF. The THF used was the same as that used as solvent in the GPC. The viscometer and THF were thermostated at 30°C with control to $\pm 0.02^\circ\text{C}$ for fifteen minutes before any measurements were made. An aspirator was used to draw the solvent up the capillary tube, just above the top calibration mark. The suction was released and the timer started as the liquid level passed the first mark and the timer stopped when the level reached the second mark. This process was repeated three times and the average time was taken if the flow times did not vary by more than 0.003 minutes. For greater variations, the process was repeated and in some cases the viscometer recleaned until consistent results were obtained.

The viscometer was dried, rinsed with the first polymer solution to be tested, then filled with about 10 cc of the solution. The same process was used to obtain flow times as was just described for pure solvent. Since the ratio of flow time of solution to flow time of pure solvent is equal to η/η_0 , the value of $\left[\ln (\eta/\eta_0) / C \right]$ could be obtained at each concentration. A plot of log viscosity number vs. concentration extrapolated to zero concentration gave the intrinsic viscosity of each sample. A typical plot is shown in figure A. 4. The solvent flow time was

FIG. A.4

VISCOSITY NUMBER - CONCENTRATION



checked after each new polymer sample was run and was constant within 0.001 minutes.

To obtain the Mark-Houwink constants a plot of $\log [\eta]$ vs. $\log M$ was made for the standard samples. This plot is shown in figure A. 5.

The equation relating $[\eta]$ and M from this plot is

$$\log [\eta] = -1.868 + 0.700 \log M$$

or

$$[\eta] = 1.36 \times 10^{-2} M^{0.70}$$

Benoit⁽¹⁵⁾ et al working with polystyrene - THF obtained the Mark-Houwink equation:

$$[\eta] = 1.41 \times 10^{-2} M^{0.70} \quad \text{which compares}$$

very well with this work.

A summary of the measured viscosities for the standards is given in table A.2.

FIG. A.5

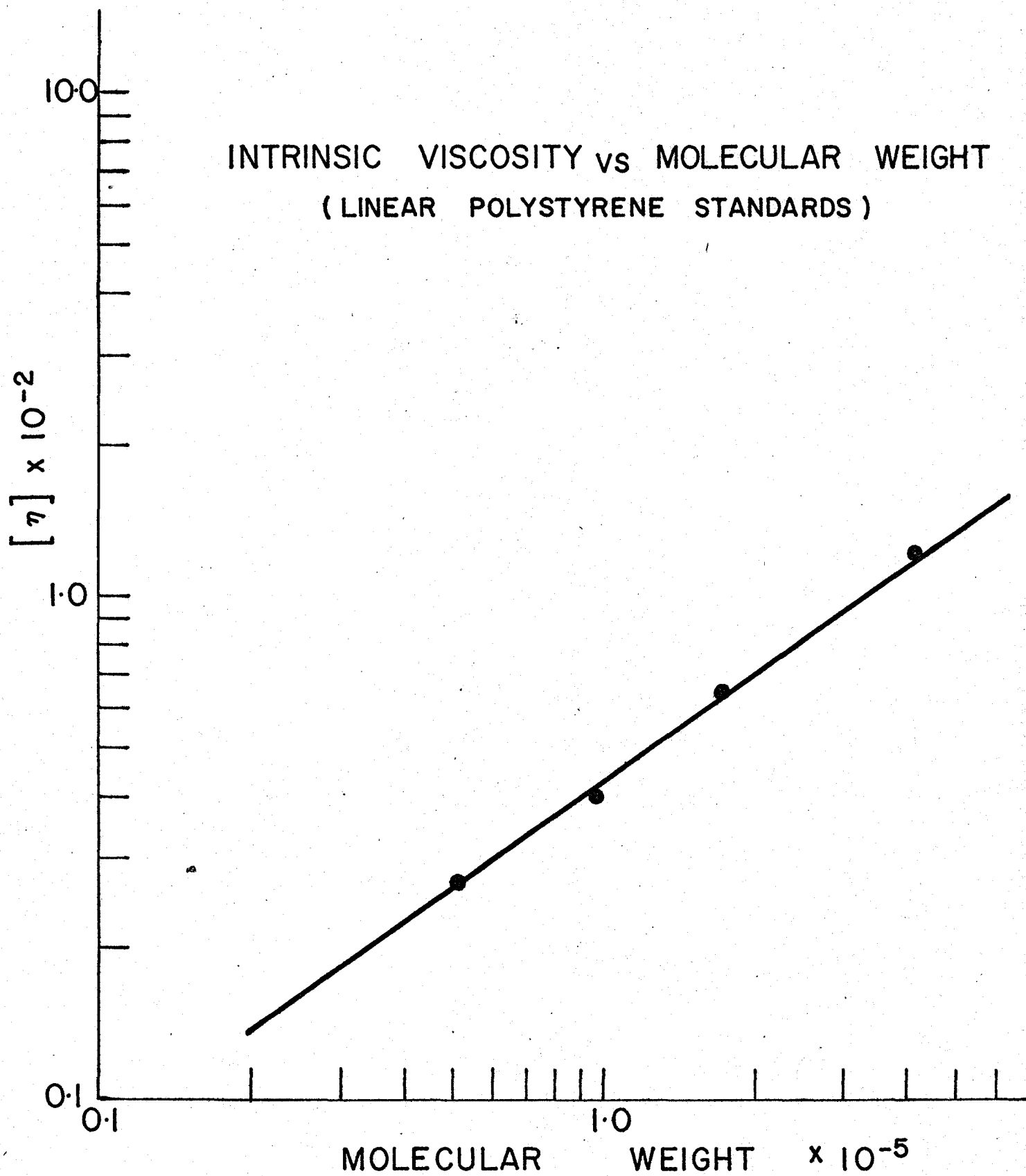


TABLE A.2

MEASURED INTRINSIC VISCOSITY OF STANDARD SAMPLES

<u>Sample code</u>	<u>Mol. wt.</u>	\bar{M}_w/\bar{M}_n	<u>Measured $[\eta]$</u>	$[\eta]M$
3 a	$\bar{M}_v = 411,000$	< 1.06	120	4.93×10^7
41984	$M = 171,000$	< 1.06	63	1.08×10^7
4 a	$(\bar{M}_v + \bar{M}_w)/2$ $= 97,200$	< 1.06	40	3.89×10^6
7 a	$\bar{M}_v = 51,000$	< 1.06	27	1.38×10^6

The intrinsic viscosities of several irradiated samples were obtained in the same manner as the polystyrene standards and molecular weights were calculated assuming the Mark-Houwink equation was valid. These data are shown in section 5.

A. 5. 3 Universal Calibration Curve

Benoit⁽¹⁵⁾ and others have shown that the GPC elution peak for a branched polymer will in general be different than that for a linear polymer of the same molecular weight. The elution peak is determined by the hydrodynamic volume of the polymer in the chromatograph column and hydrodynamic volume is a function of molecular weight and branching. Benoit⁽¹⁵⁾ showed that a plot of $[\eta] M$ against peak elution volume would yield a universal calibration curve thus giving the value of M for any material if $[\eta]$ was known. Since the elution peaks of the standard samples used for intrinsic viscosity measurements were well known on the

GPC, it was a simple matter to plot the universal calibration curve for the range of molecular weights covered by the standards. This curve is shown in figure 5.7. Using the GPC data for the irradiated samples and the measured intrinsic viscosities, the molecular weights from the universal calibration curve were calculated and compared with the data from the regular GPC calibration curve in table 5.7.

A. 5.4 Osmometry

When a pure solvent and a solution are separated by a barrier which is permeable only to solvent molecules, the difference in chemical potential between the solvent and solution will cause the pure solvent molecules to try and pass through the membrane into the solution. This may be prevented by applying a pressure to the solution side of the membrane which is called the osmotic pressure (π). For very dilute solutions, the relationship

$\pi V_1 = -RT \ln x_1 = RTx_2$ is valid, where V_1 is the molar volume of the solvent and x_1 and x_2 are the mole fractions of solvent and solute respectively. If the solute concentration tends to zero, then

$$x_2 \approx \frac{C_2 V_1}{M_2}$$

where M_2 is the molecular weight of the solute and C_2 is the concentration of solute in gram/cm³ of solution. It follows, therefore, at infinite dilution that

$$\left(\frac{\pi}{C_2}\right)_0 = \frac{RT}{M_2}$$

If the osmotic pressure is measured at several concentrations, and π/C_2 is extrapolated to zero concentration, it is then possible to determine the molecular weight of the solute (M_2).

A. 5. 4. 1 Experimental

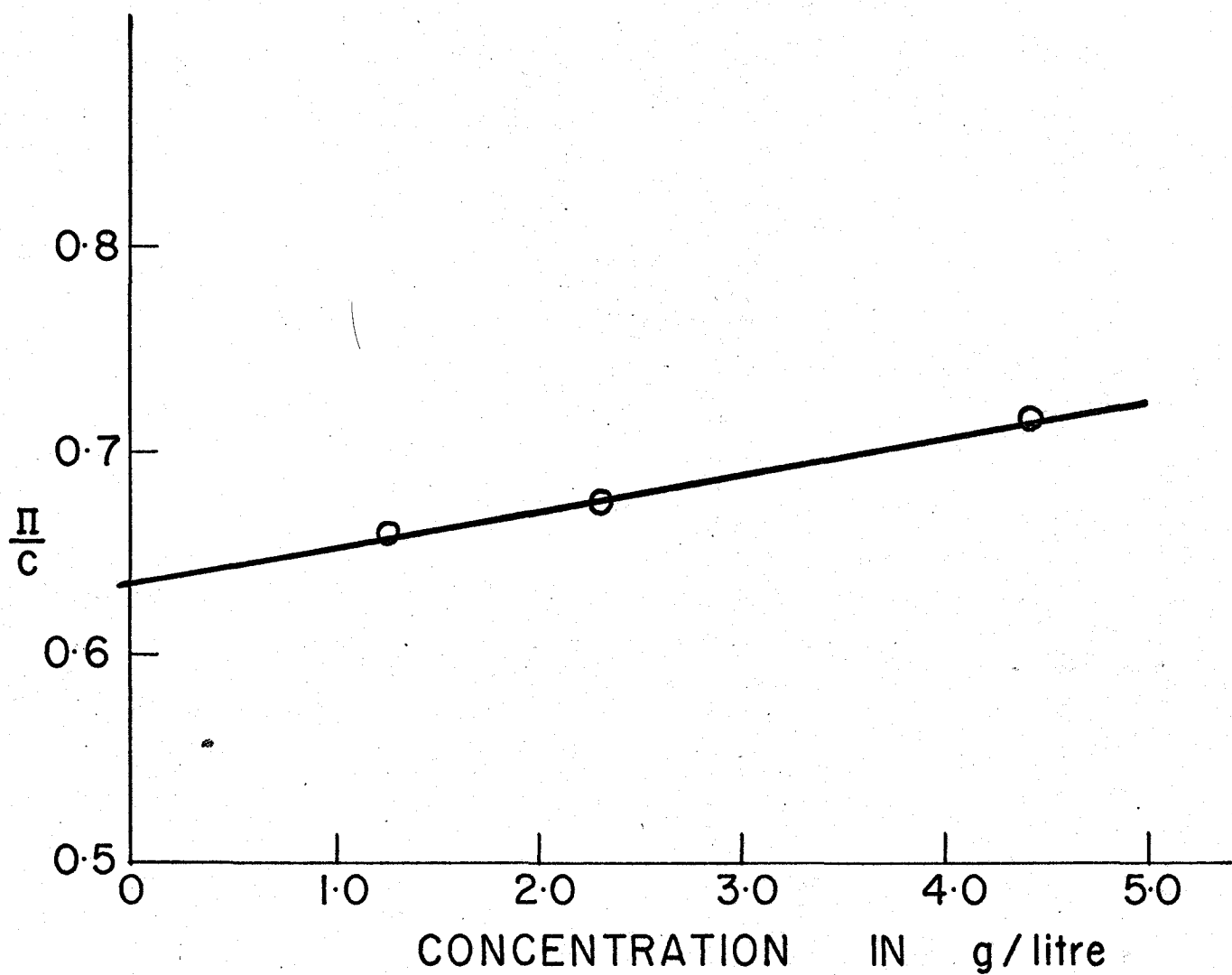
Samples for osmometry were prepared by making approximately 0. 5, 0. 25, and 0. 125 percent solutions of polystyrene in xylene. A known weight of polymer was placed into a 2 ml weighing bottle and a known amount of xylene was added. The bottles were flame sealed to prevent solvent loss while awaiting use in the osmometer.

The osmometer used was a Hewlett-Packard Model 502, high speed membrane osmometer with a Gel Cellophane 600 membrane. All measurements were made at 35°C.

To make a measurement, the weighing bottles were broken open and the sample tube of the osmometer flushed with 0. 1 to 0. 2 ml of solution. A sample of approximately 0. 2 ml was then injected into the osmometer and left for about twenty to thirty minutes until the pressure stabilized. The osmotic pressure in millimeters of water was read directly from a digital reader. Three values of π/C were plotted for each sample and extrapolated to zero concentration. A typical plot is shown in figure A. 6. The calculated values of \bar{M}_n are compared with other values of \bar{M}_n in table 5. 7.

FIG. A.6

OSMOTIC PRESSURE - CONCENTRATION



APPENDIX B

DOSIMETRY

The amount of energy per unit mass received by a body exposed to ionizing radiation is called the absorbed radiation dose. The recommended unit of absorbed dose is the rad which is defined as 100 ergs/gram. (See section 2.1) Most of the early methods used to determine this energy were based upon the measurement of the ionization produced in air by the radiation, and although experimentally this measurement is fairly simple, in general it is not easy to establish the relation between ionization in air and energy absorbed by the exposed body. Where possible it is preferable to determine the absorbed dose directly in the absorbing medium, i. e. absolute dosimetry. Calorimetric methods of dosimetry have been used for this purpose since they provide a direct measure of the absorbed energy in fundamental energy units. However, a major difficulty with this technique arises from the fact that the energy dissipated from most sources is quite small and extremely sensitive microcalorimetric methods are necessary if accurate results are to be obtained. This usually means that elaborate, time consuming, techniques are required which are not suitable for routine dosimetry measurements.

Once the strength of a radiation source has been determined by absolute methods, it is possible to use secondary indicators for measuring the relative dose. If these indicators are simple to use and respond quantitatively to changes in radiation dose while showing constancy of response over a wide range of intensities, then the relative dose can be determined on a routine basis. Cobalt glass dosimeters and

Fricke solution are two such secondary indicators that fulfill these requirements, illustrating colourimetric and chemical dosimeter methods respectively.

B.1 Cobalt Glass Dosimetry

The magnitude of the change in the visible absorption of most coloured glasses when exposed to fairly high doses of gamma radiation (10^5 to 10^7 rads) makes them suitable for dosimetry work. The dark blue coloured cobalt glasses are especially suitable in this regard since they are fairly sensitive to changes in dose, and fading after irradiation is less than that observed in non-cobalt glasses (43). Typically, a cobalt glass of the silicate glass type might contain approximately 0.5% by weight of cobalt oxide although glasses with up to 16% of cobalt oxide have been investigated and are highly sensitive to gamma radiation.

The change in the optical density of the glass after irradiation can be related to the radiation dose once the strength of the radiation source has been well defined. Plots of change in optical density vs radiation dose are usually made at different wave lengths. For maximum sensitivity, shorter wave lengths are used, but for high doses the measurements are made at longer wave lengths.

Energy absorption in one system can be related to energy absorption in another system by comparing the "stopping power" or energy absorption coefficients of the two systems. If the dose rate D_A for system A is required and the dose rate D_B for system B is known, then

$$D_A = D_B \left(\frac{\mu}{\rho} \right)_A \left(\frac{\rho}{\mu} \right)_B$$

will relate the two dose rates, where $\left(\frac{\mu}{\rho}\right)$ is the mass energy absorption coefficient of each system.

Mass energy absorption coefficients for any material are a function of the photon energy of the radiation. For cobalt glass these values range from 0.562 for 65 keV energy to 0.143 for 1,235 keV energy.

In practice, a small piece of cobalt glass is placed in a special holder in a spectrophotometer and its absorbance or transmittance measured at two or three different wave lengths, depending upon what data are available for relating the change in optical density to the radiation dose. The glass is then irradiated for 10 to 30 min. in the position at which the measurement of absorbed dose is required and the absorbance of the irradiated glass again determined. The change in absorbance or optical density is then related to absorbed dose, and from the total time of irradiation the dose rate can be determined. To minimize errors due to fading of the glass the measurement of absorbance of the irradiated sample should be taken at some fixed, convenient time after irradiation, such as one hour.

B. 1. 1 Experimental

The cobalt glasses used were Bausch and Lomb dosimeters measuring approximately 15 mm long, 6 mm wide and 1.5 mm thick. All optical measurements were made on a Beckman Model DK recording spectrophotometer using a time constant of 0.2 and a 30 minute scan time. The change in absorbance of each irradiated glass was determined using a non-irradiated glass to

set the base line and another non-irradiated glass in the reference beam. Measurements were made approximately one and one-half hours after irradiation.

The samples were held for irradiation by taping the bottom edge of the glass to a small rod which was designed to fit in the same position as the reaction vials (see figure A.2).

The Co^{60} source was brought into place with the remote handling devices and the start of the "time of irradiation" was taken at this point. When the total time had elapsed the source was removed and the samples taken for analysis on the spectrophotometer.

The translation of changes in optical density to absorbed dose were made using graphs prepared by J. M. Gebicki⁽⁴⁴⁾. The total dose in these plots was determined by Fricke dosimetry, hence the dose values obtained are all equivalent to an absorbed dose in water.

The actual sample times used and corresponding dose rates are given in table B. 1

TABLE B. 1

DOSE RATE FROM COBALT GLASS DOSIMETRY

<u>Total Irradiation Time of Sample (Min.)</u>	<u>Wave Length of Measurement (Å)</u>	<u>Total Absorbed* Dose in Rads x 10⁻⁵</u>	<u>Dose Rate (Rads / sec) x 10⁻²</u>
5	4000	0.70	2.36
	4500	0.72	2.36
	5300	0.80	2.66
15	4000	1.90	2.11
	5300	2.30	2.56
30	5300	3.70	2.06

* Calculated from graphs given by Gebicki⁽⁴⁴⁾.

Since the total absorbed dose is fairly high the measurement at 5300 Å is preferred to the shorter wave lengths. Furthermore, since a "make-ready" time of approximately one to two minutes was involved for each sample, during which time the radiation source was being put into position or taken away, the samples with short irradiation times are more likely to be in error.

It was, therefore, decided to take the result measured at 5300 Å for the 30 minute sample giving a dose rate of 2.06×10^2 rads/sec.

B.2 Fricke Dosimetry

The only chemical dosimeter in general use by the radiation chemist is the ferrous sulphate system named the "Fricke dosimeter". A brief description of this system follows, although a more detailed account is given by Swallow⁽⁴⁵⁾. When solutions of ferrous ions are irradiated, oxidation to the ferric state occurs. If ^{60}Co gamma rays, hard X-rays, fast electrons or hard β - particles are used, the G value of the reaction is 15.5 . The concentration of ferric ions is most conveniently determined spectrophotometrically at 304 m μ and can be converted to absorbed dose using the formula:

$$\text{Absorbed dose (rads)} = 2.94 \times 10^4 (1 - 0.007 t) \text{ O. D.}$$

where O. D. = optical density of irradiated solution at 304 m μ

measured in 1 cm cells and,

$t = T - 20^\circ$ where T is the temperature in $^\circ\text{C}$ at which the

O. D. is measured.

The Fricke system yields very accurate results if the total dose is between 1×10^{18} eV/gram and 2.4×10^{18} eV/gram i. e. approximately 1.6×10^4 to 3.8×10^4 rads. All irradiation cells and vessels containing the solution must be very clean and especially free of any organic material, (removed by distilling the water for the solution from potassium permanganate). It is also important to have sufficient oxygen present in the irradiation cell to complete the reaction.

B.2.1 Experimental

A Fricke solution was prepared consisting of approximately

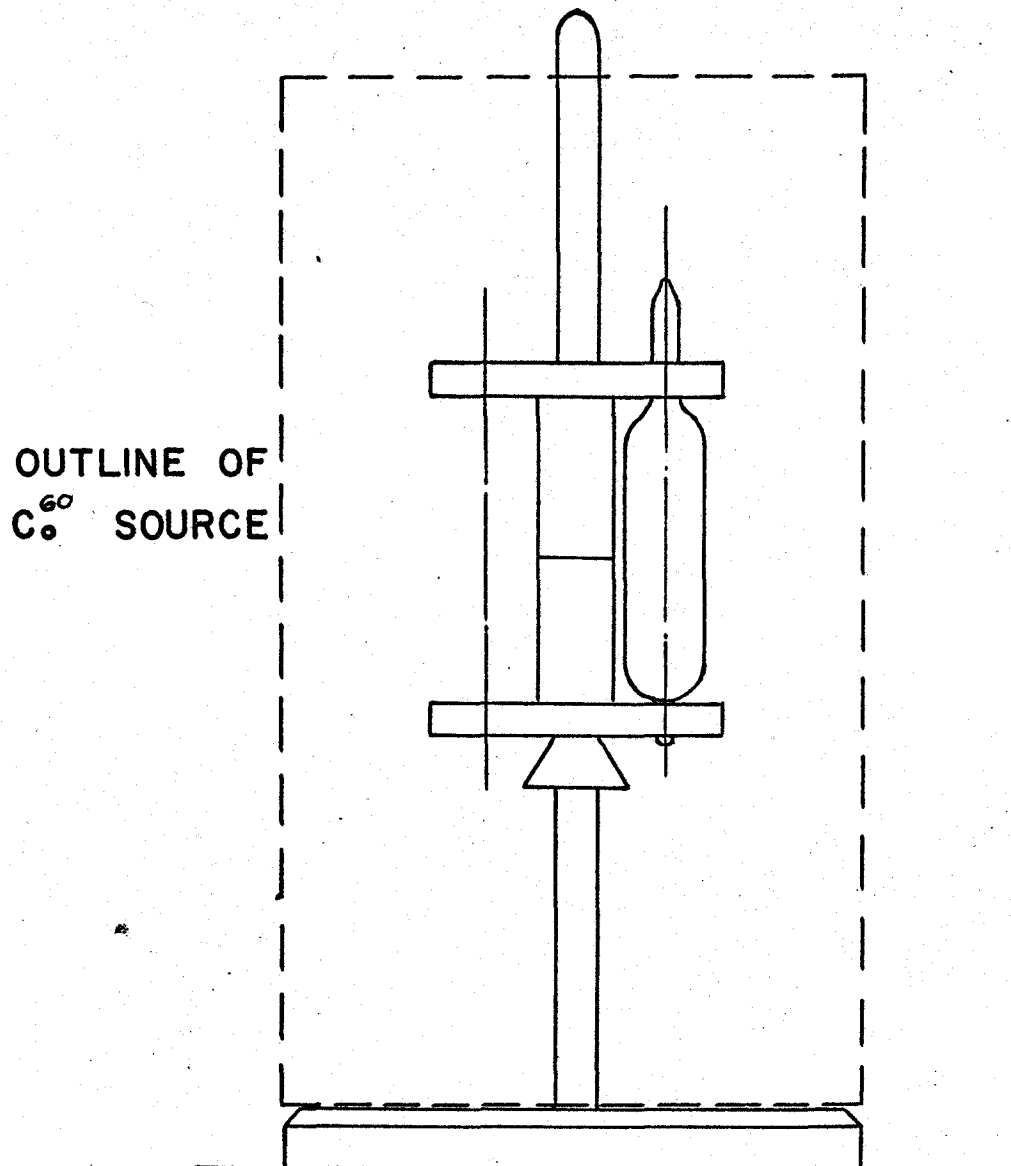
10^{-3} M ferrous ammonium sulphate in 0.1 N sulphuric acid and containing about 10^{-3} M NaCl. The water used was obtained by double distillation from an alkaline permanganate solution, which was prepared by adding a few pellets of NaOH to 0.1 N KMnO_4 . Oxygen was bubbled through the Fricke solution for several hours to be sure the solution was oxygen saturated before it was stored in a brown, glass stoppered bottle.

Identical vials to those used for the polymerization reaction were thoroughly cleaned and filled with 10 cc of the Fricke solution. They were then placed in a special holder so that they would be in the same position within the radiation source as the styrene samples. From the cobalt glass dosimetry the source strength was known to be approximately 2.06×10^2 rads/sec which required that the Fricke solution be exposed for a maximum time of 190 secs and preferably somewhat less than that so it would not receive more than the allowable maximum dose. Since the "make ready" time for moving the source was much greater than the total desired exposure time, a special technique for irradiating the Fricke solution was devised.

The special holder for the vials is shown in figure B. 1, together with the accompanying stand for centering the holder. With the radiation source out of the room, the holder, with vials in place was concealed behind a wall of lead blocks with

FIG. B. 1

VIAL HOLDER FOR FRICKE DOSIMETRY



the centering stand on the opposite side. The source was placed on the stand with remote handling devices and when it was in place the holder with the vials was lifted from behind the lead blocks with the slave manipulators, and quickly dropped into place in the centre of the source. After 100 sec. of exposure the vials were removed from the source and placed behind the lead wall while the source was removed from the room. Total "make ready" time by this technique was less than 10 sec. The process was repeated using a 120 sec. exposure time.

The absorbance of each irradiated sample was determined on the Beckman DK spectrophotometer by scanning the sample from 310 $m\mu$ to 300 $m\mu$ and using the reading at 304 $m\mu$. Non-irradiated Fricke solution was run between each irradiated sample to reset the base line. The results are given in table B.2.

TABLE B.2

DOSE RATE FROM FRICKE SOLUTION DOSIMETRY

<u>Total Irradiation Time of Sample (sec.)</u>	<u>Wave Length of Measurement (A)</u>	<u>Total Absorbed Dose in Rads x 10⁻⁴</u>	<u>Dose Rate in (Rads/sec) x 10⁻²</u>
120	3040	2.24 *	1.87
100	3040	2.00 *	2.0
			Avg. 1.94

* Average of three readings.

The short irradiation time for the Fricke solutions makes this measurement more vulnerable to errors than the cobalt glass dosimetry in spite of the fact that it is capable of much greater precision. The estimated probable error in the dose rate is about five percent. Considering that the value of the dose rate determined by each method is close and that both methods have advantages and disadvantages, the actual dose rate used is the average of the two, that is 2.0×10^2 rads/sec absorbed dose in water.

To calculate the absorbed dose in styrene it is necessary to know the value of the mass energy absorption coefficient for styrene and for water and to use the equation given on page 84. For a given photon energy, the mass energy absorption coefficient for any compound $X_m Y_n$ is given by:

$$\left(\frac{\mu}{\rho}\right)_{X_m Y_n} = m W_x \left(\frac{\mu}{\rho}\right)_x + n W_y \left(\frac{\mu}{\rho}\right)_y$$

where $\left(\frac{\mu}{\rho}\right)_x$, and $\left(\frac{\mu}{\rho}\right)_y$ are the mass energy absorption coefficients

of elements X and Y, W_x and W_y are the weights of elements X and Y divided by the total molecular weight of the compound, and m and n represent the number of times each element occurs in the compound.

The value of $\left(\frac{\mu}{\rho}\right)$ for some elements and compounds is given by Werezak (46).

For styrene (C_8H_8) the value of $\left(\frac{\mu}{\rho}\right)_{\text{styrene}} = 0.02876$

For water $\left(\frac{\mu}{\rho}\right)_{H_2O} = 0.02970$

Then the absorbed dose in styrene is given by:

$$D = 2.00 \times 10^2 \times \frac{0.02876}{0.02970} = 1.94 \times 10^2 \text{ rads/sec.}$$

All theoretical calculations for conversion of monomer to polymer in this thesis are based on a dose rate of 1.94×10^2 rads/sec.

APPENDIX C

SOLUTION OF KINETIC EQUATIONS

The theoretical conversion of monomer to polymer as a function of time, and the molecular weight distribution are given by equations (25) to (30). In the development of these equations, certain simplifying assumptions were made to permit the equations to be solved. These assumptions, and the details of the computer solution will be discussed more fully in this appendix.

C.1 Conversion - Time Curve

The rate of change of monomer concentration as a function of time is given by equation (18)

$$R = -\frac{d[M]}{dt} = k_p [R^\bullet] [M] \quad (18)$$

where $[R^\bullet]$ represents the total free radical concentration, that is total active centres where monomer could react. In a system where the production of free radicals in dead polymer molecules is at least as likely to occur as the production of monomer free radicals, the term $[R^\bullet]$ must include both monomer and polymer free radicals. From the steady state assumption we have $[R^\bullet]$ proportional to the square root of the rate of initiation,

$$[R^\bullet] = k_t^{-1/2} R_i^{1/2}$$

thus the rate of initiation must include both monomer and polymer. This is shown in equation (23) where,

$$R_{i_t} = (\phi_m [M] + \phi_p [P]) I_R \quad (23)$$

or in terms of the G_R value for monomer and polymer

$$R_{i_t} = \left[\frac{G_R^m (\text{MF}) + G_R^p (\text{PF})}{1.095 \times 10^9} \right] I_R$$

where MF and PF are monomer and polymer weight fraction.

The use of the constant 1.095×10^9 for both G_R^m and G_R^p assumes the density of monomer and polymer is the same and although this is not strictly true it is justifiable since the errors in determining G_R^m and G_R^p are greater than the error in the density approximation.

Although equation (25) will give the theoretical conversion curve when the presence of polymer is not considered or if the G_R^p value is zero, it must be modified when G_R^p and polymer concentration are appreciable to the form:

$$\ln \frac{[M_2]}{[M_1]} = - \frac{k_p}{k_t^{1/2}} \left[\frac{\{G_R^m (\text{MF}) + G_R^p (\text{PF})\} I_R}{1.095 \times 10^9} \right]^{1/2} (t_2 - t_1) \quad (34)$$

Writing equation (34) in this form assumes of course that the term

$$\frac{k_p}{k_t^{1/2}} \left[\frac{\{G_R^m (\text{MF}) + G_R^p (\text{PF})\} I_R}{1.095 \times 10^9} \right]^{1/2}$$

is constant over the interval from t_1 to t_2 . The inaccuracy of this assumption depends upon the magnitude of the time interval. The theoretical conversions presented in this thesis use a time interval of 2000 secs.

C.2 Viscosity Correction for k_t

The need to correct k_t for changes in the viscosity of the system was discussed in section 3.6. The relation between viscosity and conversion was determined experimentally as shown in section 5.2, and correlated by the equation:

$$\ln \mu = 0.694 + 12.66 (\text{PF})$$

where μ is the bulk viscosity in centipoises and PF the polymer weight fraction. Using this equation it is possible to calculate the viscosity of the system as the reaction proceeds although the validity of the expression is questionable above 45% conversion.

The relation between k_t and viscosity is more difficult to determine. Hui (29), studying the catalyzed polymerization of styrene, made a computer search for the best correlation between catalyst efficiency and k_t as a function of viscosity (assuming k_p constant over the range) and reported the following equation for calculating the change in k_t with changing viscosity:

$$\log (k_t / k_{ti}) = -0.133 \log (1 + \mu) - 0.0777 \left\{ \log (1 + \mu) \right\}^2$$

For his high conversion model he was able to predict conversion to within five per cent for viscosities as high as 3000 centipoises, although he stated that further work was required to elucidate the kinetics at viscosities above 1000 centipoises. Since Hui was studying solution polymerization these higher viscosities were attained at conversions above sixty-five or seventy percent whereas the viscosity in the bulk system is above 1000 centipoises at fifty percent conversion. It would be expected, therefore, in this study that the k_t - viscosity function would have to be modified, and as shown in section 6.1.1, this was accomplished by changing slightly the coefficient of the second degree viscosity term.

C.3 Molecular Weight Distributions

The concentration of polymer free radicals is given by equations (26) and (27). Equation (27) has the additional term $k_{ip} [P_r]$ to account for the initiation of free

radicals in dead polymer of chain length r . The constant k_{ip} is assumed independent of chain length although this need not be the only method of handling the polymer initiation. If, as an example, a polymer consisting of fifty monomer units is considered then it seems reasonable to assume that the number of possible sites for free radicals to form would be equal to the number of possible sites in fifty individual monomer molecules. If the G_R value of the polymer and the monomer were the same then the rate of initiation of free radicals in polymer P_r would be

$$R_{ip} = k_i r [P_r] \quad (35)$$

where k_i is given by

$$k_i = \frac{R_i^{\bullet}}{[M]} = \frac{G_R^m I_R}{1.095 \times 10^9 [M]} \quad (36)$$

When the G_R value of monomer and polymer were different, then k_i could be multiplied by an appropriate factor. Thus, if the G_R value of the polymer were three times greater than G_R for monomer (as has been estimated (35)) then the rate of initiation in polymer molecules would be three times greater and the term $k_{ip} [P_r]$ from equation (27) would be given by:

$$k_{ip} [P_r] = (3) k_i r [P_r] = \frac{(3) G_R^m I_R}{1.095 \times 10^9 [M]} r [P_r] \quad (37)$$

The change of concentration of dead polymer $[P_r]$ with time is given by equation (28). The term $1/2 k_{tc} \sum_{n=1}^{r-1} [R_n^{\bullet}] [R_{r-n}^{\bullet}]$ in this equation is actually a simplification since the equations from which it was derived would yield a slightly more complex form. These equations are given below:

Reaction	Rate of P_r formation (neglecting transfer)
$R_1^\bullet + R_1^\bullet \rightarrow P_2$	$\frac{dP_2}{dt} = k_{tc} [R_1^\bullet] [R_1^\bullet]$
$R_2^\bullet + R_1^\bullet \rightarrow P_3$	$\frac{dP_3}{dt} = k_{tc} [R_2^\bullet] [R_1^\bullet]$
$R_3^\bullet + R_1^\bullet \rightarrow P_4$	$\frac{dP_4}{dt} = k_{tc} [R_3^\bullet] [R_1^\bullet] +$
$R_2^\bullet + R_2^\bullet \rightarrow P_4$	$k_{tc} [R_2^\bullet] [R_2^\bullet]$
$R_4^\bullet + R_1^\bullet \rightarrow P_5$	$\frac{dP_5}{dt} = k_{tc} [R_4^\bullet] [R_1^\bullet] +$
$R_3^\bullet + R_2^\bullet \rightarrow P_5$	$k_{tc} [R_3^\bullet] [R_2^\bullet]$
$R_5^\bullet + R_1^\bullet \rightarrow P_6$	$\frac{dP_6}{dt} = k_{tc} [R_5^\bullet] [R_1^\bullet] +$
$R_4^\bullet + R_2^\bullet \rightarrow P_6$	$k_{tc} [R_4^\bullet] [R_2^\bullet] +$
$R_3^\bullet + R_3^\bullet \rightarrow P_6$	$k_{tc} [R_3^\bullet] [R_3^\bullet]$
$R_6^\bullet + R_1^\bullet \rightarrow P_7$	$\frac{dP_7}{dt} = k_{tc} [R_6^\bullet] [R_1^\bullet] +$
$R_5^\bullet + R_2^\bullet \rightarrow P_7$	$k_{tc} [R_5^\bullet] [R_2^\bullet] +$
$R_4^\bullet + R_3^\bullet \rightarrow P_7$	$k_{tc} [R_4^\bullet] [R_3^\bullet]$
etc.	etc.

To handle these equations the summation term should take the form

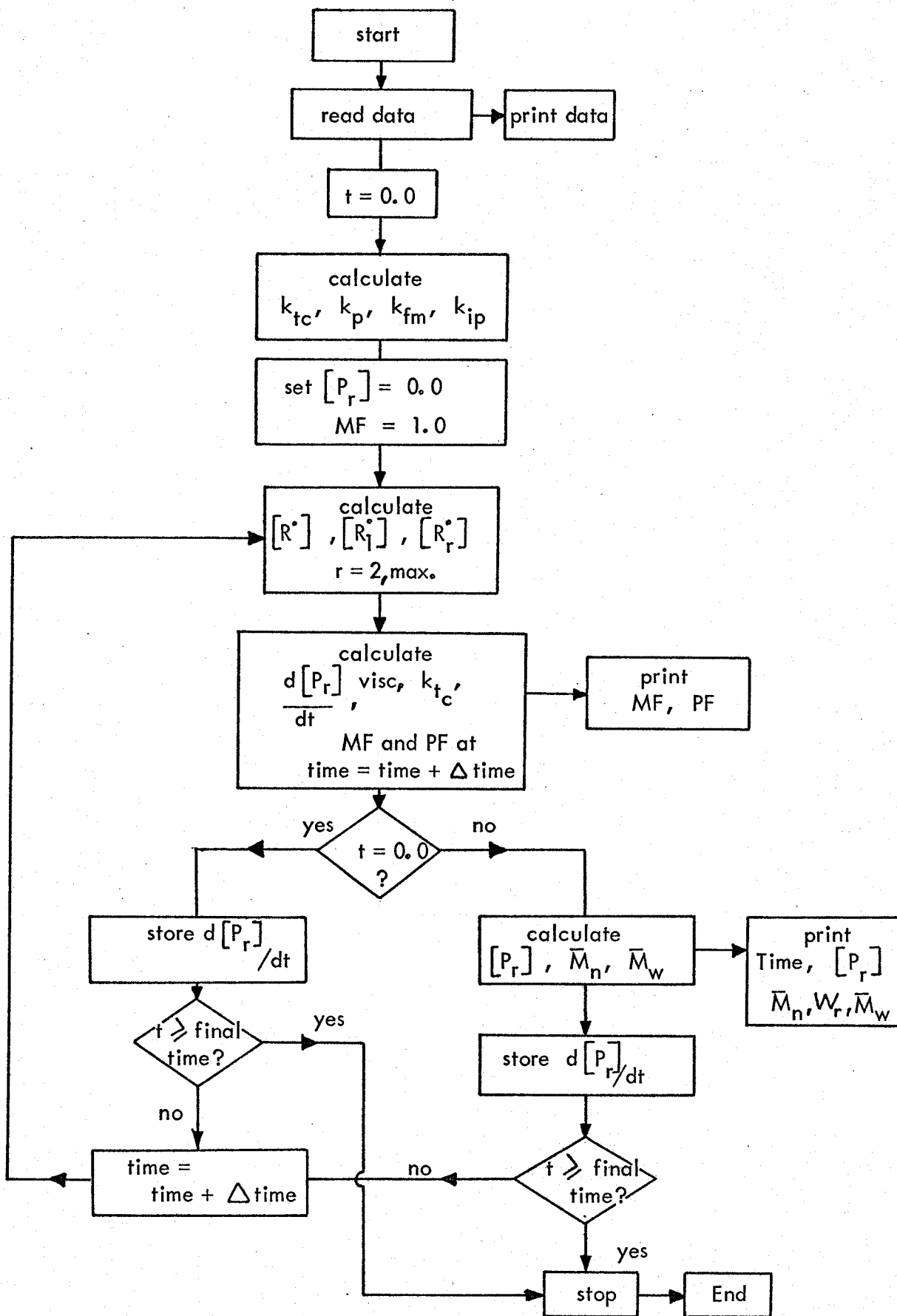
$$k_{tc} \sum_{n=1}^{r/2} [R_n^\bullet] [R_{r-n}^\bullet] \quad \text{where } r \text{ starts at } 2 \text{ and where}$$

only integer values are allowed for the term $r/2$. For example, when $r = 3$, $r/2 = 1$, when $r = 4$, $r/2 = 2$, when $r = 5$, $r/2 = 2$, etc.

A flow diagram for the solution of the molecular weight distribution equations is given in figure C. 1. Initially the value of $[P_r]$ in equation (27) is set equal to zero since $[P_r]$ is unknown. Once a value of $[P_r]$ has been calculated, that is at the end of one time interval, that value is used for the next calculation of $[R_r]$. This of course introduces an error into the calculation of $[R_r]$ since it is always using a value of $[P_r]$ from a previous time interval. However, this error is minimal if the time interval is small.

The solution of equation (28) was carried out using a modified form of the trapezoidal rule. At time t_1 the value of $d[P_r]/dt$ was determined for $r = 1$ to $r = \max$ where the maximum value is about 2000 i. e. a molecular weight of 208,000. The time is increased to t_2 and all values of $d[P_r]/dt$ are recalculated. For each value of r there will now be two points on the $d[P_r]/dt$ vs t curve. The average value of these points multiplied by the time increment will give the area under this curve i. e. $[P_r]$ at time t_2 . This procedure is repeated for consecutive time intervals up to the maximum reaction time being considered.

Logic Diagram for Radiation Reactor Program



APPENDIX D

COMPUTER PROGRAMS

```

C
C
C
C
C
C*****
C  MODEL FOR MOLECULAR WEIGHT DISTRIBUTION IN POLYSTYRENE WITH
C  INITIATION BY GAMMA RADIATION.
C*****
C
C
C  VISCOSITY CORRECTIONS MADE FOR KT
C  INITIATION OF POLYMER CONSIDERED
C
C  VARIABLES DEFINED
C
C  BMI  INITIAL MONOMER CONCENTRATION IN MOLES/LITRE
C  TEMP REACTION TEMPERATURE IN DEGREES KELVIN
C  AIR  DOSE RATE IN RADS/SEC
C  NR   MAXIMUM NO. OF MONOMER UNITS IN POLYMER
C  DELT TIME INCREMENT IN SECS
C  FACT A FACTOR TO INCREASE POLYMER INITIATION RATE
C  TIMET TOTAL TIME OF REACTION
C  GRM,GRP G VALUE OF MONOMER AND POLYMER
C  DIMENSION R(3000),DP(3000),DPX(3000),P(3000),DELH(3000),AVGS(3000)
C  DIMENSION WAITF(3000),WFRAC(3000)
C  READ(5,600)BMI,TEMP,AIR,C1
C  READ(5,601)NR,DELT,FACT,TIMET
C  READ(5,602)AKTC1,AKTC2,AKP1,AKP2,AKFM1,AKFM2
C  READ(5,603)GRM,GRP
C  WRITE(6,700)BMI,TEMP,AIR
C  WRITE(6,701)NR,DELT,TIMET
C  WRITE(6,702)AKTC1,AKTC2,AKP1,AKP2,AKFM1,AKFM2
C  WRITE(6,703)GRM,GRP
C
C  AKTCI=AKTC1*EXP(-AKTC2/TEMP)
C  AKP=AKP1*EXP(-AKP2/TEMP)
C  AKFM=AKFM1*EXP(-AKFM2/TEMP)
C  AKTC=AKTCI
C  RI=(GRM*AIR)/C1
C  AKIP=(RI*FACT)/BMI
C  WRITE(6,706)AKTCI,AKP,AKFM,AKIP,RI
C
C  BMF=1.0
C  BPF=0.0
C  BM=BMI
C  TIME=0.0
C  DO 60 I=1,NR
C  P(I)=0.0
60 CONTINUE
5  RR=((GRM*BMF+GRP*BPF)*AIR)/(C1*AKTC)**0.5
  DENO=AKP*BM+AKFM*BM+AKTC*RR
  R(1)=(RI+AKFM*BM*RR)/DENO
  DO 10 I=2,NR
  R(I)=(AKP*BM*R(I-1)+AKIP*P(I)*FLOAT(I))/DENO
10 CONTINUE
C  CALCULATION OF CHANGE IN DEAD POLYMER CONC. WITH TIME FOR EACH
C  CHAIN LENGH
C  DP(1)=AKFM*BM*R(1)

```



```

DO 300 I=2,NR
PRODI=0.0
KK=I/2
DO 400 N=1,KK
JJ=I-N
PROD=R(N)*R(JJ)
SUM=PROD+PRODI
400 PRODI=PROD
300 DP(I)=AKFM*BM*R(I)+AKTC*SUM-AKIP*FLOAT(I)*P(I)
BM=BM*EXP(-AKP*RR*DELT)
BPF=(BMI-BM)/BMI
BMF=BM/BMI
WRITE(6,709)BPF,BMF
C CALCULATION OF VISCOSITY IN CPS FROM POLYMER FRACTION VS VISCOSITY
C EXPERIMENTAL DATA
C
VISC=EXP(0.694+12.66*BPF)
C
CORRECTION OF AKTC FOR VISCOSITY
C
AKTC=AKTCI*10.0**(-0.133*ALOG10(1.0+VISC)-0.0250*(ALOG10(1.0+
1VISC))**2)
C
IF(TIME.EQ.0.0)GO TO 40
WFSUM=0.0
DO 200 J=1,NR
AVGS(J)=(DPX(J)+DP(J))/2.0
DELH(J)=AVGS(J)*DELT
P(J)=DELH(J)+P(J)
WAITF(J)=FLOAT(J)*P(J)
WFSUM=WAITF(J)+WFSUM
200 CONTINUE
WRITE(6,704)TIME,WFSUM
WRITE(6,705)(J,P(J),J=1,NR,100)
DO 800 J=1,NR
WFRAC(J)=WAITF(J)/WFSUM
800 CONTINUE
WRITE(6,710)(J,WFRAC(J),J=1,NR,100)
C
CALCULATION OF NUMBER AND WEIGHT AVERAGES
C
TOTL=0.0
ASUM=0.0
BSUM=0.0
DO 100 I=1,NR
SIGMA=P(I)*FLOAT(I)
TOTL=SIGMA+TOTL
ASUM=P(I)+ASUM
WAIT=SIGMA*FLOAT(I)
100 BSUM=WAIT+BSUM
AVMN=(TOTL/ASUM)*104.0
AVMW=(BSUM/TOTL)*104.0
WRITE(6,707)AVMN,AVMW
C
40 DO 500 J=1,NR
DPX(J)=DP(J)
500 CONTINUE
C
IF(TIME.GT.TIMET)GO TO 50

```

TIME=TIME+DELT

GO TO 5

50 CONTINUE

C

600 FORMAT(3F7.2,E11.4)

601 FORMAT(I8,3F9.1)

602 FORMAT(3(E11.4,F8.1))

603 FORMAT(2F6.3)

700 FORMAT(5X,22H INITIAL MONOMER CONC=,F5.2,5X,6H TEMP=,F7.2,
15X,11H DOSE RATE=,F7.2)701 FORMAT(5X,19H MAX MONOMER UNITS=,I4,5X,15H TIME INTERVAL=,F9.1,
15H SECS,5X,12H TOTAL TIME=,F9.1,5H SECS)

702 FORMAT(3(E11.4,F8.1))

703 FORMAT(5X,17H G VALUE MONOMER=,F6.3,5X,17H G VALUE POLYMER=,F6.3)

704 FORMAT(10X,6H TIME=,F9.1,5H SECS,5X,23H WEIGHT FRACTION TOTAL=,
1E12.4)

705 FORMAT(5X,6(2HP(,I4,2H)=,E12.3))

706 FORMAT(5X,5E12.3)

707 FORMAT(5X,19H NUMBER AVG MOL WT=,E12.4,10X,19H WEIGHT AVG MOL WT=,
1E12.4)709 FORMAT(5X,22H POLYMER WT. FRACTION=,E12.3,5X,22H MONOMER WT. FRACT
1ION=,E12.3)

710 FORMAT(2X,6(3HWF(,I4,2H)=,E11.3))

STOP

END

CD TOT 0142

 DIGITAL TRANSLATOR PROGRAM FOR GPC INTERPRETATION

THIS PROGRAM WAS WRITTEN BY WATERS ASSOCIATES AND THE POLYMER
 GROUP MCMASTER UNIVERSITY - MAY 1967 -
 MODIFIED BY S. BALKE, M MCMASTER UNIVERSITY 1968

CONVERSION PROGRAM FROM DIGITIZER DATA TO BASE CORRECTED
 HEIGHT DATA AT PREDETERMINED INTERVALS ALSO CONTAINS DATA
 READ-IN, HEADING READ-IN, AND CONVERTED PRINTOUT)

THIS PROGRAM IS CONDUCTED WITH F-FIELD

CALNO IS CALIBRATION CODE NUMBER
 CONC IS CONCENTRATION OF SAMPLE IN PERCENT
 DIFFH IS DIFFERENTIAL HEIGHT AFTER CORRECTION FOR BASE LINE CHANGE
 FLOW IS FLOW RATE OF ELUTING SOLVENT IN ML/MIN
 JCBBAS IS BEGINNING OF BASE IN COUNTS
 JCBCAL IS BEGINNING OF CALCULATION IN COUNTS
 JCECAL IS END OF CALCULATION IN COUNTS
 JCEBAS IS END OF BASE IN COUNTS
 CINTV IS INTERVAL OF PRINT-OUT IN COUNTS
 JD IS INPUT DATA, TIME OR HEIGHT
 JHBBAS IS HEIGHT AT BEGINNING OF BASE
 JHEBAS IS HEIGHT AT END OF BASE
 RTIME IS INTERVAL OF GPC INPUT READING IN SECONDS
 KA, NH ARE COUNTERS FOR GPC CURVE
 KSETS GREATER THAN ZERO TO GIVE MORE PRINTOUTS FOR DEBUGGING
 M IS CONTROL NUMBER, 0-HEIGHT,1-HEADING,4-INJECTION,7-ELUTION
 N IS DATA NUMBER FROM GPC INPUT
 NCURVE IS NUMBER OF CURVE TO BE CALCULATED
 NB IS NUMBER OF OUTPUT DATA POINTS AFTER CALCULATION
 NE IS TOTAL NUMBER OF INPUT DATA POINTS
 NHEAD IS IDENTIFICATION HEADING NUMBER
 NUM1,NUM2 ARE NUMBERS TO CONTROL GPC INPUT FORMAT
 SAM1,SAM2 IS SAMPLE NUMBER
 TINJ IS INJECTION TIME IN SECONDS

COMMON NCURVE , JCEBAS

COMMON M, JD, KK

REAL JCBBAS, JCEBAS, JHBBAS, JHEBAS, JHT, JY, JZ, JH1, JH2, JCBCAL, JCECAL
 REAL JHH2

DIMENSION HCT(400), TWORT(400), TWOLT(400)

DIMENSION JC(2400), M(2400), JD(2400), JCBBAS(40), JCBCAL(40),

1 JHEAD(40), JCECAL(40), JCEBAS(40), RTIME(40), FLOW(40),

2 CINTV(40), JHT(400), COUNT(400), CTITPL(400), DIFFH(400),

3 SAM2(40), NHEAD(40), SAM1(40), CALNO(40), TINJ(40),

4 CONC(40), DATE1(40), DATE2(40), SOLVNT(40), TEMP(40)

DIMENSION STV(400)

```

C   READ IN HEADING DATA
C
  READ(5,11) NCURVE,NIDELT,KSETS
  READ(5,76) CALV,CORV
  CTRATO = CALV/CORV
  WRITE(6,2150) NCURVE,NIDELT,KSETS,CALV,CORV,CTRATO
2150  FORMAT(1H0,3I5,3F10.5)
C   WHEN INTERVAL OF PRINTOUT IS 0.05 THEN...
C   NIDELT=4, CORRESPONDS TO A PUNCH OUT EVERY 0.25 OF A CT.
C   =3.....EVERY 0.20 CT.
C   = 2 ..... EVERY 0.15 CT
C   = 1 .....EVERY 0.10 CT
76   FORMAT(5F8.5)
      READ(5,12) (NHEAD(I),SAM1(I),SAM2(I),CALNO(I),SOLVNT(I),DATE1(I),
1     DATE2(I),      TINJ(I),RTIME(I),CONC(I),FLOW(I),TEMP(I),
2     CINTV(I),JCBBAS(I),JCBCAL(I),JCECAL(I),JCEBAS(I),I=1,NCURVE)
C
C ECHO CHECK ON HEADING DATA
      WRITE(6,13)
      WRITE(6,14) (NHEAD(I),SAM1(I),SAM2(I),CALNO(I),SOLVNT(I),DATE1(I),
1     DATE2(I),      TINJ(I),RTIME(I),CONC(I),FLOW(I),TEMP(I),
2     CINTV(I),JCBBAS(I),JCBCAL(I),JCECAL(I),JCEBAS(I),I=1,NCURVE)
C
C   READ IN GPC DATA
C
      CALL DATRD
      NE = KK
      IF ( NE . LT. 2400 )   GO TO 3
      WRITE(6,4)
3     CONTINUE
C
C   ECHO CHECK ON GPC DATA
      WRITE(6,910)
      WRITE(6,911) (M(I),JD(I),I=1,NE)
C
380   N=0
      NK=0
      KA=0
      NH=1
C
C   BEGIN REPETITIVE CALCULATION PROGRAM FOR EACH CURVE
C
371   LA=0
      KC=0
      NB=0
      LC=0
      JX=0
      LB=0
      KD=0
      KB=0
      LD=0
300   N=N+1
      IF(N-NE) 381,382,382
381   IF(M(N)-1) 300,301,302
301   IF(LD-1) 350,351,300
C
C   FIRST HEADING RECORDED
350   KA=KA+1

```

```
JHEAD(KA)=JD(N)
LD=1
C
C   HEADING SEARCH TO FIND DATA
DO 499 NH=1,NCURVE
IF (NHEAD(NH)-JHEAD(KA)) 499,498,499
499 CONTINUE
WRITE(6,916) N
KA=KA-1
LD=0
GO TO 300
C
498 IF (KSETS.EQ.0) GO TO 300
WRITE(6,901) NHEAD(NH)
GO TO 300
C
302 IF(M(N)-4) 303,303,304
303 IF(LD-1) 405,601,601
405 WRITE(6,906) N
GO TO 300
601 IF(LC-1) 320,300,300
C
C   FIRST INJECTION RECORDED
C
320 LA=1
LC=1
GO TO 300
C
C   SECOND HEADING NOTED - LOCATION STORED
C
351 NHEAD2=N
LD=2
GO TO 300
C
C   COUNT ELUTIONS TO END OF BASE READING
C
304 IF(LA-1) 300,305,306
305 JC(N)=JX+1
JX=JC(N)
IF (FLOAT(JX)-JCBBAS(NH)) 300,313,313
313 JBBAS=JC(N)
LA=2
NA=N
314 N=N+1
IF(M(N)-1) 315,314,314
315 JHBBAS=JD(N)
N=NA
GO TO 316
306 JC(N)=JX+1
JX=JC(N)
IF(LB-1) 316,307,308
316 IF (FLOAT(JX)-JCBCAL(NH)) 300,312,312
312 NBCAL=N
LB=1
GO TO 300
307 IF (FLOAT(JX)-JCECAL(NH)) 300,311,311
311 NECAL=N
LB=2
```

```

IF (KSETS.EQ.0) GO TO 318
WRITE(6,825)
WRITE(6,830) N,NH,JC(N),JCBBAS(NH),JCBCAL(NH),JHBBAS,JCECAL(NH),
1 JCEBAS(NH)
318 N=N-1
GO TO 300
308 IF (FLOAT(JX)-JCEBAS(NH)) 300,309,309
309 JEBAS=JC(N)
N=N-1
IF(M(N)-1) 310,309,309
310 JHEBAS=JD(N)
IF (KSETS.EQ.0) GO TO 319
WRITE(6,830) N,NH,JC(N),JCBBAS(NH),JCBCAL(NH),JHBBAS,JCECAL(NH),
1 JCEBAS(NH),JHEBAS
WRITE(6,835)

C
C INTERPOLATE FOR HEIGHT DATA
C
319 N=NBCAL
JTELB=JD(N)
JX=JC(N)
NIX=NBCAL+1
NN=N

C WRITE OUT CONVERTED DATA
C
WRITE(6,901) NHEAD(NH)
DO 200 N=NIX,NECAL
IF(M(N)-1) 330,200,331
330 KB=KB+1
JHT(KB)=JD(N)
GO TO 200
331 IF(M(N)-7) 200,332,332
332 JTELE=JD(N)
KC=KB
NIY=KD+1
DO 100 KQ=NIY,KC
CT1=100*(KQ-KD)-JTELB
CT2=100*(KC-KD)-JTELB+JTELE
COUNT(KQ)=CT1/CT2+FLOAT(JX)
JHH2 = (JHEBAS-JHBBAS)*(COUNT(KQ)-JCBBAS(NH))/(JCEBAS(NH)-
1 JCBBAS(NH))
HCT(KQ)=JHT(KQ)-JHH2-JHBBAS
COUNT(KQ)=COUNT(KQ)*CTRATO
WRITE(6,10000) COUNT(KQ), HCT(KQ)
10000 FORMAT(1H , 2F16.3)
100 CONTINUE
JX=JC(N)
KD=KC
JTELB=JTELE
200 CONTINUE
N=NN

C
C INTERPOLATE TO PREDETERMINED COUNT INTERVALS
C
JCBBAS(NH)=JCBBAS(NH)*CTRATO
JCBCAL(NH)=JCBCAL(NH)*CTRATO
JCECAL(NH)=JCECAL(NH)*CTRATO
JCEBAS(NH)=JCEBAS(NH)*CTRATO
C

```

```

NB=1.
CTITPL(1)=JCBCAL(NH)
JY=JHT(1)
JZ=COUNT(1)

```

C

```

K1C=KC
WRITE(6,902) SAM1(NH),SAM2(NH),CALNO(NH),TINJ(NH),CONC(NH),
1 DATE1(NH),DATE2(NH),SOLVNT(NH),TEMP(NH),FLOW(NH),NK
WRITE(6,903) JCBBAS(NH),JCEBAS(NH),JCBCAL(NH),JCECAL(NH),
1 CINTV(NH),RTIME(NH)
WRITE(6,10002)
10002 FORMAT(1H0,5X,6HCOUNTS,10X,5HTWOLT,10X,5HTWORT,10X,6HLINEAR)
DO 400 KB=1,KC
IF (CTITPL(NB)-COUNT(KB)) 334,334,333
333 JY=JHT(KB)
JZ=COUNT(KB)
IF (KSETS.EQ.0) GO TO 400
WRITE(6,840) KA,NH,KB,JHT(KB),JY,JZ,COUNT(KB),NB,CTITPL(NB),JH1,
1 JH2,DIFFH(NB),JCBBAS(NH),JHBBAS,JCEBAS(NH),JHEBAS
GO TO 400
334 JH1=((JHT(KB)-JY)*(CTITPL(NB)-JZ))/(COUNT(KB)-JZ)
JH2=((JHEBAS-JHBBAS)*(CTITPL(NB)-JCBBAS(NH)))/(JCEBAS(NH)-
1 JCBBAS(NH))
DIFFH(NB)=JY+JH1-JHBBAS-JH2
CALL INTERP (K1C,COUNT,HCT,CTITPL(NB),H2LT,H2RT)
TWORT(NB)=H2RT
TWOLT(NB)=H2LT
WRITE(6,10001) CTITPL(NB),TWOLT(NB),TWORT(NB),DIFFH(NB)
10001 FORMAT(1H,5F16.4)
IF (KSETS.EQ.0) GO TO 338
WRITE(6,840) KA,NH,KB,JHT(KB),JY,JZ,COUNT(KB),NB,CTITPL(NB),JH1,
1 JH2,DIFFH(NB),JCBBAS(NH),JHBBAS,JCEBAS(NH),JHEBAS
338 IF (DIFFH(NB).LT.0.) DIFFH(NB)=0.0
NB=NB+1
CTITPL(NB)=CTITPL(NB-1)+CINTV(NH)
IF (CTITPL(NB).LT.COUNT(KB)) GO TO 334
JY=JHT(KB)
JZ=COUNT(KB)
IF (CTITPL(NB)-JCECAL(NH)) 400,400,335
400 CONTINUE
335 NK=NB
DO 2010 ICHECK=1,NK
ST=DIFFH(ICHECK)
STV(ICHECK)=ST
2010 CONTINUE
NKMID=3
TEMMID=TWOLT(3)
DO 2006 IMID=4,NK
IF(TWOLT(IMID).LE.TEMMID)GO TO 2006
TEMMID=TWOLT(IMID)
NKMID=IMID
2006 CONTINUE
C
NKTEMP=NK
NK=NK+4
N1K = NK
NDELT=0
DO 2002 ICOR=5,NK

```

```

NCOR=ICOR-4+NDEL
NDEL=NDEL+N1DEL
DIFFH(ICOR)=TWOLT(NCOR)
IF(NCOR.GE.NKMID) DIFFH(ICOR)=TWORT(NCOR)
IF(DIFFH(ICOR).LT.0.)DIFFH(ICOR)=STV(NCOR)
DIFFH(5)=STV(NCOR)
IF(DIFFH(ICOR).LT.0.) DIFFH(ICOR)=0.
XP=DIFFH(ICOR)
IF(XP.GT.0.0) GO TO 2002
IF(NCOR.LT.NKMID)GO TO 2002
N1K=ICOR
N2K=NCOR
GO TO 2005
2002 CONTINUE
2005 NK=N1K
DO 2001 IZERO = 1,4
DIFFH(IZERO)=0.
2001 CONTINUE
XNDE=N1DEL
VO=CTITPL(1)-(4.*((XNDE*CINTV(NH))+CINTV(NH)))
VF=CTITPL(N2K-5)+5.*CINTV(NH)
WRITE(7,599)NHEAD(NH)
599 FORMAT(I5)
WRITE(7,811) VO,VF
811 FORMAT(8X,2F8.3)
WRITE(7,810) (DIFFH(INK),INK=1,NK)
DO 500 NB = 1, NK
500 DIFFH ( NB ) = 0.0
NK=NKTEMP
C
C RECYCLE TO START OF PROGRAM
C
IF (LD-1) 371,371,370
370 N=NHEAD2-3
GO TO 371
C
C
1 FORMAT(12(1X,I1,I3))
4 FORMAT(1H0,20X,14H TOO MUCH DATA)
11 FORMAT(3I5)
12 FORMAT(I5,6A5/5A5,5F5.1)
13 FORMAT (1H0,26HECHO CHECK ON HEADING DATA / 1X,26(1H-)/)
14 FORMAT (1H ,/(5X,I5,5X,2A5,10X,A5,5X,A5,10X,2A5 / 5X,A5,5X,A5,
1 5X,A5,5X,A5,5X,A5,5F10.1 // ) )
800 FORMAT (3F10.4,I10 )
810 FORMAT(8F10.3)
815 FORMAT (I5,2X,2A5,2X,4A6,3X,15X,2A5 )
820 FORMAT(1H ,8I15)
825 FORMAT (1H0,6X,2H N,5X,3H NH,5X,3H JC,2X,7H JCBBAS,1X,7H JCBCAL,
1 1X,7H JHBBAS,1X,7H JCECAL,1X,7H JCEBAS,1X,7H JHEBAS /)
830 FORMAT (1H ,3I8,6F8.1)
835 FORMAT (1H0,5X,3H KA,5X,3H NH,5X,3H KB,4X,4H JHT,5X,3H JY,5X,
1 3H JZ,2X,7H COUNTS,4X,3H NB,2X,7H CTITPL,4X,4H JH1,4X,4H JH2,
2 1X,7H DIFFH,1X,7H JCBBAS,1X,7H JHBBAS,1X,7H JCEBAS,1X,7H JHEBAS,
3 /)
840 FORMAT (1H ,3I8,2F8.1,2F10.3,I4,F8.3,7F8.1 )
901 FORMAT (1H1,131(1H*)/45X,26H GPC IDENTIFICATION NUMBER,I5/
1 1X,131(1H*)/)

```



```

902 FORMAT (1H0,16X,13HSAMPLE NUMBER,9X,2A5/12X,18HCALIBRATION NUMBER,
1 5X,A5/15X,15H INJECTION TIME,5X,A5,9H SECONDS/16X,14H CONCENTRAT
2ION,F10.2,9H PERCENT/25X,5HMONTH,5X,A5/ 27X,3HDAY,5X,A5/25X,
3 22X,8H SOLVENT,5X,A5/ 18X,12H TEMPERATURE,5X,A5,
410H DEGREE C/ 20X,10H FLOW RATE,5X,A5,10H ML./MIN. /12X,
5 18H TOTAL DATA POINTS ,5X, I5 )
903 FORMAT (1H0,11X,18H BEGINNING OF BASE,F10.1,8H COUNTS /
1 18X,12H END OF BASE ,F10.1,8H COUNTS / 5X,25H BEGINNING OF CALC
2ULATION ,F10.1,8H COUNTS / 11X,19H END OF CALCULATION,F10.1,
3 8H COUNTS / 9X,
4 21H INTERVAL OF PRINTOUT,F10.3,1X,7H COUNTS / 9X,21H REPEAT TIM
5E INTERVAL,F10.0,1X,8H SECONDS /// )
904 FORMAT (1H0,10X,37(1H*),23H CALCULATED DATA OUTPUT,2X,37(1H*)//
1 20X, 18H DATA POINT NUMBER, 15X,7H COUNTS,18X,24H CURVE HEIGHT AB
2OVE BASE / )
905 FORMAT (1H ,I30,F30.3,F30.1 )
906 FORMAT( 1H0, 43H INJECTION NOT PRECEDED BY MATCHED HEADING,5X,
1 12H DATA NUMBER,2X,I4)
910 FORMAT ( ///1X, 22HECHO CHECK ON GPC DATA / 1X,22(1H-) //)
911 FORMAT ( 24(1X,I1,I3) )
916 FORMAT( 1H0, 20H HEADING NOT MATCHED , 5X, 12H DATA NUMBER ,2X,I6)

```

```

382 STOP
END

```

```
$IBFTC DATRD
```

```
SUBROUTINE DATRD
```

```

C THIS DECK READS THE TRANSLATED BINARY CARDS AND CONVERTS EACH
C WORD INTO THE TWO WORDS M(K) AND JD(K) .
C IT ALSO IGNORES THE SECOND PIECE OF INFORMATION IF TWO HEADINGS ,
C ELUTIONS , OR INJECTIONS OCCUR CONSECUTIVELY.
C THE DATA IS READ FROM THE FIRST PIECE UNTIL THE LAST JCEBAS.

```

```

REAL JCEBAS
COMMON NCURVE , JCEBAS(40)
COMMON M, JD, KK
DIMENSION M(2400) , JD(2400) , I(12)
NHD = 0
INJ = 0
ELUT = 0.0
K = 1
DO 21 JJ = 1,199
3 CALL READNO(I,N)
WRITE(6,25) (I(J) , J = 1,N)
25 FORMAT( 1H0, 12I5)
DO 2 J= 1,N
M(K) = I(J) /1000
JD(K) = I(J) - M(K)* 1000
IF( K. EQ. 1) GO TO 23
KJ = K- 1
IF( M(K) . EQ . M(KJ) . AND. M(K) . NE . 0) GO TO 2
23 IF ( M(K) . EQ . 1 ) NHD = NHD + 1
IF ( NHD . LT . NCURVE ) GO TO 22
IF ( M(K) . EQ . 4 ) INJ = 1
IF ( M(K) . EQ . 7 . AND . INJ . EQ . 1 ) ELUT = ELUT + 1.
IF ( ELUT . EQ . JCEBAS(NCURVE) ) GO TO 4
22 K = K+1
2 CONTINUE
21 CONTINUE
4 KK = K+1

```

```

RETURN
END
$IBMAP BINCRD
REM READNO READS BINARY CODED CARDS WITH THE FOLLOWING
REM FORMAT. INFORMATION STARTS IN COLUMN 4 AND ENDS
REM EITHER IN COLUMN 75 OR WITH TWO SUCCESSIVE BLANKS.
REM IN ANY COLUMN PUNCHES 12-3 SHOULD NOT OCCUR
REM A NUMBER 0-9 IS CODED IN BINARY IN ROWS 6-9 WITH
REM PUNCHES IN ROWS 4 AND 5. A SPACE IS JUST A PUNCH IN
REM ROW 4. ANY OTHER PUNCH IS ILLEGAL AND RESULTS IN
REM AN ERROR MESSAGE BEING PRINTED AND A WORD COUNT OF
REM ZERO BEING RETURNED.
REM CALLING SEQUENCE IS CALL READNO(I,N) WHERE
REM ONE CARD IS READ AND N WORDS ARE RETURNED IN I(1),
REM I(2),... I(N).
REM IF A $CARD IS READ THE PROGRAM GIVES A MESSAGE AND
REM EXIT IS CALLED.
REM IF A BCD CARD IS READ, ANOTHER MESSAGE IS GIVEN AND
REM N IS SET TO -1.
REM THE ROUTINE COUNTS THE CARDS IT READS AND USES
REM THIS COUNT IN ALL THE ERROR MESSAGES.
ENTRY READNO
EXTERN JOBIN,JOBOU
READNO SAVE 1,2,4
CLA 4,4
STA N
STZ* N
CLA 3,4
SUB =1
STA I
STZ TEMP
CDCNT AXT 0,1
TXI *+1,1,1
SXA CDCNT,1
MSM FINSW
CALL JOBIN
TPL HELLO TROUBLE
AXT -1,4
SXA RDPOI,4
SSP
ADD =25
AXT 6,1
STA PCS,1
TIX *-1,1,1
AXT 24,2
MSP SWITCH ODD AND EVEN CHARACTERS DIFFER
WDLOOP AXT 6,1
CHLOOP ZAC
XEC PCS,1
SWITCH BRN GOOD
TZE JOIN
ERROR STZ* N ERROR
CLA CDCNT
TSX S.XDVA,4
STQ MESS+4
CALL JOBOU(BAD1)
RETURN READNO
BAD1 PZE 1

```

	PTW	MESS,,5	
MESS	BCI	5,ILLEGAL PUNCH IN CARD	
GOOD	PAX	,4	
	TXL	STORE,4,0	
	TXL	ERROR,4,31	
	TXL	STORE,4,32	
	TNX	ERROR,4,47	
	TXI	*+1,4,-1	
	TXH	ERROR,4,9	
	SXA	CHAR,4	
	LDQ	=10	
	VLM	TEMP,,4	
	LLS	4	
	ADD	CHAR	
	STO	TEMP	
JOIN	CLS	SWITCH	
	STO	SWITCH	
	TIX	CHLOOP,1,1	
	TIX	WDLOOP,2,1	
	MSP	FINSW	
STORE	CLA	TEMP	
	TNZ	*+2	
	RETURN	READNO	
RDPOI	AXT	** ,4	
I	STO	** ,4	
	TXI	*+1,4,-1	
	SXA	RDPOI,4	
	CLA*	N	
	ADD	=1	
N	STO	**	
	STZ	TEMP	
FINSW	BRA	JOIN	
	RETURN	READNO	
HELLO	CAS	*+2	
	TRA	DOLCRD	
	PON	**	CAN'T OCCUR
	CLS	=1	
	STO*	N	
	CLA	CDCNT	
	TSX	S.XDVA,4	
	STQ	MES+1	
	CALL	JOBOU(BAD2)	
	RETURN	READNO	
BAD2	PZE	1	
	PTW	MES,,5	
MES	BCI	5, CARD	IS A BCD CARD
DOLCRD	PAX	,2	
	SXD	POINT,2	
	CAL	POINT	
	TSX	S.SCCR,4	
	TMT	14	
	TSX	S.SCCR,4	
	MSM	S.SCDI	
	CLA	CDCNT	
	TSX	S.XDVA,4	
	STQ	MEZ+1	
	CALL	JOBOU(BAD3)	
	TRA	S.JXIT	

```

BAD3  PZE      1
      PTW      MEZ,,4
MEZ    BCI      4,CARD      IS A $CARD.
POINT PZE      S.SAVE,,**
      PCS      **,2,0
      PCS      **,2,1
      PCS      **,2,2
      PCS      **,2,3
      PCS      **,2,4
      PCS      **,2,5
PCS    EQU      *
CHAR   PZE      **
TEMP   PZE      **
      END

```

```

$IBFTC INTERP
SUBROUTINE INTERP (JK,X,Y,XA,YA,ZA)
DIMENSION X(400),Y(400)
M1=2
M11=1
602  YA=0.0
     IF((X(1)-X(2)).GT.0.0) GO TO 804
     DO 805 II=1,JK
     IF((XA-X(II)).LE.0.0) GO TO 806
805  CONTINUE
804  DO 809 II=1,JK
     IF((X(II)-XA).LE.0.0) GO TO 806
809  CONTINUE
806  IF(II.LE.M1) GO TO 807
     IF(II.GE.(JK-M11)) GO TO 808
     MM=II-M1+1
     MMM=II+M11
     GO TO 810
807  MM=1
     MMM=M1+M11
     GO TO 810
808  MM=JK-M1+M11-1
     MMM=JK
810  DO 801 I=MM,MMM
     PROD=Y(I)
     DO 800 J=MM,MMM
     IF(J.EQ.I) GO TO 800
     PROD=PROD*(XA-X(J))/(X(I)-X(J))
800  CONTINUE
801  YA=YA+PROD
     IF(M1.EQ.3) GO TO 601
     M1=3
     M11=0
     ZA = YA
     GO TO 602
601  RETURN
     END

```

NOMENCLATURE

C	Catalyst concentration
C_0	initial catalyst concentration
$[\eta]$	intrinsic viscosity
f	catalyst efficiency
G_R	G value of free radical production
GPC	gel permeation chromatograph
I	rate of formation of free radicals in monomer
I_R	dose-rate
k	kinetic rate constant
M_0	initial monomer concentration
$[M]$	monomer concentration in gm-moles/litre
M^\bullet	monomer free radical
MF	monomer weight fraction
MWD	molecular weight distribution
$\Phi_m [M]$	monomer free radicals produced in moles/litre/rad
$\Phi_p [P]$	polymer free radicals produced in moles/litre/rad
PF	polymer weight fraction
P_r	dead polymer of chain length r
R_i	rate of initiation of monomer or polymer
R_{it}	total rate of initiation
R^\bullet	free radical of any chain length
$[R_r^\bullet]$	concentration of free radical of chain length r in gm-moles/litre

r	subscript for number of monomer units in a polymer chain
\bar{r}_n	number average chain length
\bar{r}_w	weight average chain length
S^\bullet	solvent free radical
t	reaction time in seconds
T	absolute temperature in degrees Kelvin
μ	bulk viscosity in centipoises
W_r	weight fraction of polymer of chain length r
X	conversion of monomer to polymer

Subscripts for rate constant k

d	decomposition of catalyst
fm	transfer to monomer
fs	transfer to solvent
ip	initiation of polymer
i	where $rk_i = k_{ip}$
p	propagation
tc	termination by combination
td	termination by disproportionation
t	$k_t = k_{tc} + k_{td}$
t_i	k_{t_i} initial value of k_t

BIBLIOGRAPHY

1. Tebbens, K. , "Free Radical Polymerization of Styrene in a Batch Reactor",
Thesis, McMaster University (1966).
2. Boundy and Boyer, "Styrene - Its Polymers, Copolymers and Derivatives",
Reinhold, New York, p. 240 (1952).
3. Simon, E. , Ann. , 31, 265 - 277 (1839)
4. Boundy and Boyer, "Styrene - Its Polymers, Copolymers and Derivatives",
Reinhold, New York, p.2 (1952).
5. Blyth, J. , and Hoffman, A. W. , Ann. , 53 , 292 - 329 (1845).
6. Staudinger, H. , Ber. , 53, 1073 (1920).
7. Boundy and Boyer, "Styrene - Its Polymers, Copolymers and Derivatives,"
Reinhold, New York, p. 216 (1952).
8. Kraemer, E. O. and Lansing, W. D. , J. Phys. Chem. , 39, 156 (1935).
9. Kraemer, E. O. , and Lansing, W. D. , J. Am. Chem. Soc. 57, 1369 (1935).
10. Mark, H. , and Saito, G. , Monatsh, 68, 237 (1936)
11. Johnson, J. F. , Porter, R. S. , and Cantour, M. J. R. , Rev. in Macromolecular
Chem. 1, (2), 393 - 434 (1966).
12. Boldingh, J. , Rec. Trav. Chim. , 69, 247 (1959).
13. Vaughan, M. F. , Nature, 188, 55 (1960).
14. Moore, J. C. , Chem. Eng. News, p. 4 - 5, October, (1965) .
15. Benoit, H. , Grubisic, Z. , Rempp, P. , Duker, D. , and Zilliox, J. G. ,
Third Inter. Seminar on GPC, Geneva, Switzerland.

16. Boundy and Boyer, "Styrene - Its Polymers, Copolymers and Derivatives", Reinhold, New York, p. 324 (1952).
17. Chapiro, A. , "Radiation Chemistry of Polymeric Systems", Interscience, New York - London, Preface (1962).
18. Spinks, J.W.T. , and Woods, R. J. , "An Introduction to Radiation Chemistry," John Wiley and Sons, New York, (1964).
19. International Commission on Radiological Units and Measurements, Copenhagen, (1953); *Nucleonics* 12, No. 1, 11 (1954).
20. Chapiro, A. "Radiation Chemistry of Polymeric Systems", Interscience, New York - London, p. 15 (1962).
21. Werezak, G. N. , "Gamma Induced Chlorination of Methane" Thesis, McMaster University, p. 29 (1966).
22. Flory, P. J. , "Principles of Polymer Chemistry", Cornell Univ. Press, New York, p. 37 (1953).
23. Plesch, P. H. , "The Chemistry of Cationic Polymerization", The MacMillan Co., New York, p. 241 (1963).
24. Chapiro, A. , and Stannett, V. , *J. Chim. Phys.* 57, 35, (1960).
25. Plesch, P. H. , "The Chemistry of Cationic Polymerization", The MacMillan Co., New York, p. 646 (1963).
26. Bamford, C. H. , Barb, W. G. , Jenkins, A. D. , and Onyon, P. F. , "The Kinetics of Vinyl Polymerization by Radical Mechanisms", Butterworths, London, p. 7, (1958).

27. Bandrup, J. , and Immergent, E. H. , "Polymer Handbook", Interscience, New York - London, p. 11 - 57 (1966).
28. De Schrijver, F. , Smets, G. , J. Polymer Science, A 1, 4, 2201 (1966).
29. Hui, A. W. T. , "Free Radical Polymerization of Styrene up to High Conversion", Thesis, McMaster University (1967).
30. Chapiro, A. , and Wahl, P. , Compt. rend. , 238, 1803 (1954).
31. Chapiro, A. , Magat, M. , Sebben, J. , and Wahl, P. , International Symp. Macromol Chem. , Milan - Torino, (1954)
Ricerca Sci. Suppl. A 73 (1955).
32. Chapiro, A. , "Radiation Chemistry of Polymeric Systems", Interscience, New York - London, p. 132 - 138 (1952).
33. Ibid. p. 174.
34. Chapiro, A. , and Sebban-Danon, J. , J. Chim. Phys. 54, 763 (1957).
35. Chapiro, A. , "Radiation Chemistry of Polymeric Systems", Interscience, New York - London, p. 606 (1952).
36. Wall, L. A. , and Florin, R. E. , J. Appl. Polymer Sci. 2, 251 (1959).
37. Ballentine, D. S. , Colombo, P. , Glines, A. , and Manowitz, B. , B. N. L. 229 (T-37), 1953, Chem. Eng. Progress Symp. Series 267 (1954).
38. Landler, Y. , Thesis, University of Paris, (1952).
39. Vaughan, M. F. , Trans. Faraday Soc. , 48, 576 (1952).
40. Robertson, E. R. , Trans. Faraday Soc. , 52, 426 (1956).
41. Hodgins, J. W. , Werezak, G. N. , and Ross, S. L. Can. J. Chem. Eng. , 43, 117 - 119 June (1965).

42. Tung, L. H. , J. Appl. Polymer Sci. , 10, 375 and 1271 (1966).
43. Kreidl, N. J. , and Blair, G. E. , Nucleonics, Vol. 14, No. 1, Jan. (1956).
44. Gebicki, J. M. , "Practical Gamma Ray Dosimetry" - Unpublished report McMaster University
45. Swallow, A. J. , "Radiation Chemistry of Organic Compounds", Pergamon Press, p. 41 - 43 (1960).
46. Werezak, G. N. , "Gamma Induced Chlorination of Methane" Thesis, McMaster University, p. 215 (1966).
47. Boundy and Boyer, "Styrene - Its Polymers, Copolymers and Derivatives", Reinhold, New York, p. 315 (1952).
48. Duerksen, J. H. , "Free Radical Polymerization of Styrene in Continuous Stirred Tank Reactors", McMaster University (1968).
49. Staudinger, H. , and Heuer, W. , Ber. Dtsch. chem. Ges. 63, 222 (1930).
50. Allen, P. W. , Editor, "Techniques of Polymer Characterization", Butterworths, London, p. 173 (1959).
51. Mark, H. , Der Feste Körper, Leipzig (1938).
52. Houwink, R. , J. Pract. Chem. 157, 15 (1940).
53. Allen, P. W. , Editor, "Techniques in Polymer Characterization", Butterworths, London, p. 201 (1959).
54. Stockmayer, W. H. , and Fixman, M. , Ann. N.Y. Acad. Sci. 57, 334 (1953).
55. Volk, W. "Applied Statistics for Engineers", McGraw - Hill, New York (1958).